

Published by Faculty of Sciences and Mathematics, University of Niš, Serbia Available at: http://www.pmf.ni.ac.rs/filomat

Ulam-Hyers-Rassias stability results for nonlinear mixed partial integro-differential equations with discontinuous kernels

Rahim Shaha, Natasha Irshada, İnci M. Erhanb, Muhammad Imran Khanc

^aDepartment of Mathematics, Kohsar University Murree, Murree, Pakistan
^bDepartment of Computer Engineering, Aydın Adnan Menderes University, Aydın, Türkiye
^cDepartment of Biotechnology, Kohsar University Murree, Murree, Pakistan

Abstract. This paper presents a novel stability analysis of nonlinear mixed partial integro-differential equations with discontinuous kernels. The paper fills a significant gap in the literature by offering, for the first time, a rigorous proof of stability in both the Ulam-Hyers and Ulam-Hyers-Rassias frameworks for such equations under general conditions. Discontinuous kernels present a great deal of difficulty due to the complex behavior they introduce into the system's dynamics and their intrinsic singularities. This work not only specifies the stability criteria but also provides insights into the underlying mechanisms governing the behavior of the solution by creating a new analytical structure. This will be done by using fixed-point arguments within the framework of continuous function spaces, equipped with a generalized Bielecki metric. Additionally, in order to provide insight into the stability behavior under slight perturbations, we investigate the σ -semi-Ulam-Hyers stability of the nonlinear mixed partial integro-differential equations with discontinuous kernels. The results deepen our knowledge of partial integro-differential equations and may find use in a variety of areas where discontinuous kernels are significant. In contrast to many previous studies, our method allows the system's solution to exist in metric space instead of normed space. Furthermore, this work is innovative and significant because no previous study has been done on the stability of this kind of nonlinear mixed partial integro-differential equations with discontinuous kernels. Finally, for verification, we provide several examples and include 2D and 3D graphs of specific variables and functions, which are generated using MATLAB.

1. Introduction

Ulam–Hyers stability was first established in the twentieth century, following a seminar at the University of Wisconsin where Ulam [43] discussed a type of stability related to functional equations. Hyers subsequently solved this problem [11], and the findings have since been extensively generalized by

²⁰²⁰ Mathematics Subject Classification. Primary 26D10; Secondary 45G10, 45M10, 47H10.

Keywords. Ulam-Hyers stability, Ulam-Hyers-Rassias stability, Banach fixed-point theorem, mixed partial integro-differential equations, Bielecki metric.

Received: 30 December 2024; Revised: 19 February 2025; Accepted: 04 March 2025

Communicated by Miodrag Spalevic

^{*} Corresponding author: Rahim Shah

 $[\]label{lem:main} \begin{tabular}{l} Email\ addresses: $rahimshah@kum.edu.pk, shahraheem1987@gmail.com\ (Rahim\ Shah), natashairshad24@gmail.com\ (NatashaIrshad), incierhan@gmail.com\ (İnci\ M.\ Erhan), drimrankhan@kum.edu.pk\ (Muhammad\ Imran\ Khan) \\ \end{tabular}$

ORCID iDs: https://orcid.org/0009-0001-9044-5470 (Rahim Shah), https://orcid.org/0009-0008-8166-6520 (Natasha Irshad), https://orcid.org/0000-0001-6042-3695 (İnci M. Erhan), https://orcid.org/0000-0003-1096-1529 (Muhammad Imran Khan)

Aoki [47] and Rassias [48], who modified the control conditions that define approximate solutions. These developments in Ulam–Hyers stability have found numerous applications across fields such as physics, electronics, biology, economics, and mechanics [4, 20, 25]. The stability of functional equations, including applications to parallel electrical circuits, is further explored in [13]. Khan and colleagues [28] examined Ulam–Hyers stability using fractal–fractional derivatives with a power–law kernel, focusing on chaotic systems in circuit design. As a result, a large body of literature, including monographs [2, 49], survey articles [3, 15], and other referenced works, has been published, extending the problem and theorem in various directions and to different types of equations [26, 31].

Fixed-point theory is a fundamental concept in mathematical analysis that investigates the existence and characteristics of points that remain unchanged under a given function or mapping. Far from being merely an abstract idea, this theory has significant implications and practical applications across various fields (see, e.g., earlier studies [32–38]). A major application is in the analysis of differential and integral equations, which are used to model numerous physical processes. Fixed-point theorems, including the Banach fixed-point theorem and the Schauder fixed-point theorem, are often employed to establish the existence and uniqueness of solutions to these equations. This is particularly important in disciplines such as physics and engineering, where comprehending the behavior of systems governed by these equations is critical. Additionally, fixed-point theory underpins the mathematical framework for optimization problems, enabling the identification of equilibrium points where an objective function reaches its optimal value. This is especially relevant in areas like convex optimization, game theory, and economics, where equilibrium states, such as Nash equilibria, are viewed as fixed-points of specific mappings.

The Banach fixed–point theorem, also referred to as the contraction mapping theorem, is one of the most prominent results in fixed–point theory [5–7]. It offers a robust approach for establishing the existence and uniqueness of fixed–points within complete metric spaces. According to the theorem, if a function acts as a contraction mapping meaning it consistently reduces the distance between points by a fixed ratio in a complete metric space then there is a unique fixed–point at which the function's value equals the point itself. This theorem is fundamental not only in the study of differential and integral equations but also in the application of various iterative methods for solving equations, numerical analysis, and dynamical systems. The Banach fixed–point theorem is especially valuable because it ensures convergence to a unique solution through iterative processes, making it an indispensable tool in both theoretical and applied mathematics. Using fixed–point theory, many researchers have examined the stability of integral and differential equations over the past six decades [8, 21, 46].

Several recent studies have explored different aspects of stability in differential and integral equations. In [39], the authors investigate the Hyers–Ulam stability of Bernoulli's differential equation, extending the classical stability analysis to fundamental nonlinear equations. In [40], the authors study the Ulam–Hyers–Mittag–Leffler stability of nonlinear fractional reaction–diffusion equations with delay, providing insights into the behavior of such systems under perturbations. Further contributions are made in [41], where the authors examine the Hyers–Ulam–Rassias stability for impulsive Fredholm integral equations on finite intervals, emphasizing the role of stability in integral equations with impulsive effects. Moreover, in [42], the authors analyze the stability properties of oscillatory Volterra integral equations in the Ulam framework, highlighting their applicability in systems governed by hereditary effects. These studies collectively advance the understanding of stability in various classes of equations, offering valuable theoretical and applied perspectives.

In [51], the authors explored the stability and existence results for impulsive integro–differential equations. The Hyers–Ulam stability of higher–order nonlinear differential equations with fractionally integrable impulses was addressed in [9], which expanded on the findings from [17]. Diaz and Margolis (refer to [18]) established a well–known fixed–point theorem in a complete generalized metric space, which has been extensively applied by numerous authors (see, for instance, [27]). In 2012, K. Ciepliński provided a comprehensive survey (see [19]) on the applications of various fixed–point theories in the Hyers–Ulam stability of functional equations. J. Brzdęk (refer to [16]) presented a fixed–point theory for operators that are not necessarily linear. In 2003, researchers utilized specific fixed–point theories to examine the stability of certain functional equations (see [24, 50]) and demonstrated the Hyers–Ulam–Rassias stability. Their work integrated the research contributions of Hyers, Rassias, and Gajda [52]. Furthermore, Shah et al. (refer

to [29]) studied the stability of hybrid differential equations using Gronwall's lemma, offering a rigorous approach to stability analysis in hybrid systems. These contributions collectively enhance the understanding of various stability notions in differential and integral equations, reinforcing their role in mathematical modeling and real–world applications.

In this paper, motivated by the aforementioned studies, we explore the Ulam–Hyers stability, the Ulam–Hyers–Rassias stability, and a fresh type of stability, referred to as σ –semi–Ulam–Hyers stability, for the following nonlinear mixed partial integro–differential equation (NMPIDE) with discontinuous kernel,

$$\frac{\partial}{\partial s} \left[\frac{f(t,s) - h(t,s)}{k(\alpha(s), f(t,s))} \right] = \gamma \phi(s) \int_{a}^{b} G(t,\xi) \Psi(f(\xi,s)) d\xi, \tag{1}$$
$$f(t,a) = \mu(t),$$

with $(t,s) \in [a,b] \times [a,b] \times [a,b]$, where, for starting, a and b are fixed real numbers, $h:[a,b] \times [a,b] \to \mathbb{C}$, $\alpha:[a,b] \to \mathbb{C}$, $k:\mathbb{C} \times \mathbb{C} \to \mathbb{C}$, $\phi:[a,b] \to \mathbb{C}$, $\Psi:\mathbb{C} \to \mathbb{C}$ are continuous functions, $G:[a,b] \times [a,b] \to \mathbb{C}$ represents the singular kernel of position, $f \in C^2([a,b] \times [a,b])$, γ is a constant, and $\mu:[a,b] \to \mathbb{C}$ is the initial function.

It is straightforward to demonstrate that Equation (1) is equivalent to the integral equation

$$f(t,s) = h(t,s) + B(t)k(\alpha(s), f(t,s))$$

$$+ \gamma k(\alpha(s), f(t,s)) \int_a^s \int_a^b \phi(\tau)G(t,\xi)\Psi(f(\xi,\tau)) d\xi d\tau,$$
(2)

where

$$B(t) = \left[\frac{(\mu(t) - h(t, a))}{k(\alpha(a), \mu(t))} \right].$$

Partial integro–differential equations (PIDEs) are widely used across various domains because they can model systems that involve both differential and integral aspects. In biological studies, PIDEs help to analyze disease dynamics by incorporating how past exposures affect current infection rates, thus reflecting cumulative impacts over time. In material science, these equations are applied to describe viscoelastic materials by integrating memory effects into the stress–strain relationship, which accounts for the delayed responses to external forces. In the realm of finance, PIDEs are essential for option pricing and risk management, capturing how historical market conditions and interest rates impact financial assets. In control systems, PIDEs model processes where previous states influence current control actions, such as in adaptive control systems where past performance shapes present decisions. For signal processing, PIDEs are used to represent situations where outputs depend on the entire history of input signals, facilitating tasks such as noise reduction and data smoothing. In environmental modeling, PIDEs are employed to describe the dispersion of pollutants, considering how past concentrations and conditions affect current dispersion. These varied applications highlight the ability of PIDEs to offer a comprehensive framework for understanding systems with both immediate and historical influences (see, for instance, earlier studies [1, 12, 30], and others).

The main novelties and innovations of this manuscript are as follows:

- (1) This work is the first to establish Ulam–Hyers stability, Ulam–Hyers–Rassias stability, and a new form of stability, termed σ –semi–Ulam–Hyers stability, for nonlinear mixed partial integro–differential equations (NMPIDEs) with discontinuous kernels. Specifically, it investigates Ulam–Hyers stability, Ulam–Hyers–Rassias stability, and σ –semi–Ulam–Hyers stability over bounded intervals, as well as Ulam–Hyers–Rassias stability over unbounded intervals. While extensive studies exist for ordinary differential equations, stability analyses of partial differential equations have remained largely unexplored.
- (2) Unlike prior research, which primarily focuses on partial differential equations in normed spaces, this work develops a novel analytical framework by employing fixed–point arguments within continuous function spaces equipped with a generalized Bielecki metric. This approach significantly broadens the applicability of stability results.

- (3) The paper pioneers the study of NMPIDEs with discontinuous kernels over both bounded and unbounded intervals, addressing challenges posed by their complex dynamic behavior and intrinsic singularities.
- (4) This work not only extends classical stability results for partial differential equations but also introduces a generalized stability framework that accommodates discontinuous kernels, offering deeper insights into the stability properties of such equations.
- (5) The σ -semi–Ulam–Hyers stability provides a new perspective on how small perturbations influence the behavior of solutions, further enriching the theoretical understanding of stability in systems with memory effects and discontinuities.
- (6) The findings significantly advance the stability theory initiated by Ulam [44] by incorporating new methodological approaches and extending the results to a broader class of equations with discontinuous kernels.
- (7) To validate the theoretical results, the paper presents several illustrative examples along with 2D and 3D MATLAB–generated visualizations, offering practical insights into the stability behavior of solutions.

This paper is organized as follows: In Section 2, we review the fundamental results and concepts that form the basis for the analysis presented in the subsequent sections. Section 3 is dedicated to proving the Ulam–Hyers–Rassias stability for the NMPIDE (1) on a bounded interval. In Section 4, we establish σ –semi–Ulam–Hyers stability for NMPIDE (1) within the same interval. Section 5 further explores Ulam–Hyers stability for NMPIDE (1) on a bounded interval. Moving to Section 6, we address Ulam–Hyers–Rassias stability for NMPIDE (1) on an unbounded interval. Section 7 presents examples and simulations to illustrate the theoretical results. To conclude, Section 8 summarizes the core findings of the paper and offers suggestions for future research.

2. Preliminary Results

This section presents the notations, definitions, and fundamental concepts from the literature that will be used throughout the discussion. The definitions and theorem provided are crucial for confirming the Ulam–Hyers, Ulam–Hyers–Rassias, and σ –semi–Ulam–Hyers stabilities of the NMPIDE (1).

We will begin by revisiting the definition of a generalized metric and the Banach fixed-point theorem, which are crucial for demonstrating our results.

Definition 2.1 ([45]). Let Z be a nonempty set and $d: Z \times Z \to [0, +\infty]$ be a given mapping. We say that d is a generalized metric on Z if and only if d satisfies the following:

- d(x, y) = 0 if and only if x = y;
- d(x, y) = d(y, x) for all $x, y \in Z$;
- $d(x,z) \le d(x,y) + d(y,z)$ for all $x, y, z \in Z$.

Theorem 2.2 ([14]). *Let* (Z,d) *be a generalized complete metric space and consider a mapping* $T:Z\to Z$ *which is a strictly contractive operator, that is,*

$$d(Tx, Ty) \le K d(x, y), \quad x, y \in Z$$

for some Lipschitz constant $0 \le K < 1$. If there exists a nonnegative integer k such that $d(T^{k+1}x, T^kx) < \infty$ for some $x \in \mathbb{Z}$, then the following three propositions hold true:

• the sequence $(T^n x)_{n \in \mathbb{N}}$ converges to a fixed-point x^* of T;

- x^* is the unique fixed–point of T in $Z^* = \{ y \in Z : d(T^k x, y) < \infty \}$;
- If $y \in Z^*$, then

$$d(y, x^*) \le \frac{1}{1 - K} d(Ty, y). \tag{3}$$

Next, we present the definitions of Ulam–Hyers stability and Ulam–Hyers–Rassias stability for the NMPIDE (1).

Definition 2.3. *Let* f *be a continuous function on* $[a,b] \times [a,b]$ *such that*

$$\left| \frac{\partial}{\partial s} \left[\frac{f(t,s) - h(t,s)}{k(\alpha(s), f(t,s))} \right] - \gamma \phi(s) \int_{a}^{b} G(t,\xi) \Psi(f(\xi,s)) d\xi \right| \le \sigma(t,s),$$

$$\left| f(t,a) - \mu(t) \right| \le \sigma(t,s),$$

where $(t,s) \in [a,b] \times [a,b]$, and σ is a nonnegative function. If there is a solution f_0 of the NMPIDE and a constant K > 0, independent of f and f_0 , satisfying

$$|f(t,s)-f_0(t,s)| \leq K\sigma(t,s),$$

for all $(t,s) \in [a,b] \times [a,b]$, then we say that the NMPIDE (1) has the Ulam–Hyers–Rassias stability.

Definition 2.4. *Let* f *be a continuous function on* $[a,b] \times [a,b]$ *such that*

$$\left| \frac{\partial}{\partial s} \left[\frac{f(t,s) - h(t,s)}{k(\alpha(s), f(t,s))} \right] - \gamma \phi(s) \int_{a}^{b} G(t,\xi) \Psi(f(\xi,s)) d\xi \right| \le \theta,$$

$$\left| f(t,a) - \mu(t) \right| \le \theta,$$

where $(t,s) \in [a,b] \times [a,b]$, and $\theta \ge 0$. If there is a solution f_0 of the NMPIDE and a constant K > 0, independent of f and f_0 , satisfying

$$|f(t,s)-f_0(t,s)| \leq K\theta,$$

for all $(t,s) \in [a,b] \times [a,b]$, then we say that the NMPIDE (1) has the Ulam–Hyers stability.

Next, we will present a fresh form of stability, as developed by Castro and Simões [21], which bridges the gap between Ulam–Hyers and Ulam–Hyers–Rassias stabilities.

Definition 2.5. Let σ a nondecreasing function defined on $[a,b] \times [a,b]$. If for each continuous function f satisfying

$$\left| \frac{\partial}{\partial s} \left[\frac{f(t,s) - h(t,s)}{k(\alpha(s), f(t,s))} \right] - \gamma \phi(s) \int_{a}^{b} G(t,\xi) \Psi(f(\xi,s)) d\xi \right| \le \theta,$$

$$\left| f(t,a) - \mu(t) \right| \le \theta,$$

where $(t,s) \in [a,b] \times [a,b]$, and $\theta \ge 0$, there is a solution f_0 of the NMPIDE and a constant K > 0, independent of f and f_0 , such that

$$|f(t,s) - f_0(t,s)| \le K\sigma(t,s), \quad (t,s) \in [a,b] \times [a,b],$$

then we say that the NMPIDE (1) has the σ -semi-Ulam-Hyers stability.

3. Ulam-Hyers-Rassias Stability on a Bounded Interval

In this section, we address the necessary conditions for the NMPIDE (1) over a bounded interval $(t,s) \in [a,b] \times [a,b]$, where a and b are fixed real numbers.

We examine the space $C^2([a,b] \times [a,b])$ equipped with a generalized form of the Bielecki metric, as detailed in [22]:

$$d(f,g) = \sup_{(t,s)\in[a,b]\times[a,b]} \frac{|f(t,s) - g(t,s)|}{\sigma(t,s)},\tag{4}$$

where σ is a nondecreasing continuous function from $[a,b] \times [a,b]$ to $\mathbb{R}_+ = (0,\infty)$. For a broader scope, this paper explores a more general form of the metric.

It is important to note that $C^2([a,b] \times [a,b])$ with the generalized metric d forms a complete metric space [10], [23].

Theorem 3.1. Let $h:[a,b]\times[a,b]\to\mathbb{C}$, $B:[a,b]\to\mathbb{C}$ and $\alpha:[a,b]\to\mathbb{C}$ be continuous functions for all $(t,s)\in[a,b]\times[a,b]$ and γ be a positive constant. Assume that $k:\mathbb{C}\times\mathbb{C}\to\mathbb{C}$ is a continuous function such that there exists M>0 so that

$$M = \sup_{(t,s)\in[a,b]\times[a,b]} \left| k(\alpha(s), f(t,s)) \right|, \quad f \in \mathbb{C},$$
(5)

and $\phi:[a,b]\to\mathbb{C}$ is also continuous. Moreover, suppose that $G:[a,b]\times[a,b]\to\mathbb{C}$ represents the singular kernel of position such that there exists N>0 so that

$$\left|\phi(\tau)G(t,\xi)\right| \le N \tag{6}$$

and $\Psi: \mathbb{C} \to \mathbb{C}$ is a continuous function such that there exists L > 0 so that

$$|\Psi(f(\xi,\tau)) - \Psi(g(\xi,\tau))| \le L|f(\xi,\tau) - g(\xi,\tau)| \tag{7}$$

for all $f, g \in C^2([a, b] \times [a, b])$, and $(\xi, \tau) \in [a, b] \times [a, b]$. In addition, let $\sigma : [a, b] \times [a, b] \to \mathbb{R}_+$ be a nondecreasing continuous function such that there exists $\beta > 0$ so that

$$\int_{a}^{s} \int_{a}^{b} \sigma(\xi, \tau) \, d\xi d\tau \le \beta \sigma(t, s) \tag{8}$$

for all $(t,s) \in [a,b] \times [a,b]$.

If $f \in C^2([a,b] \times [a,b])$ is such that

$$\left| \frac{\partial}{\partial s} \left[\frac{f(t,s) - h(t,s)}{k(\alpha(s), f(t,s))} \right] - \gamma \phi(s) \int_{a}^{b} G(t,\xi) \Psi(f(\xi,s)) d\xi \right| \le \sigma(t,s), \tag{9}$$

$$|f(t,a) - \mu(t)| \le \sigma(t,s),\tag{10}$$

where $(t,s) \in [a,b] \times [a,b]$, and $\beta N \gamma L M < 1$, then there is a unique function $f_0 \in C^2([a,b] \times [a,b])$, solution of Equation (1), that is,

$$f_0(t,s) = h(t,s) + B(t)k(\alpha(s), f_0(t,s))$$

$$+ \gamma k(\alpha(s), f_0(t,s)) \int_a^s \int_a^b \phi(\tau)G(t,\xi)\Psi(f_0(\xi,\tau)) d\xi d\tau$$
(11)

such that

$$\left| f(t,s) - f_o(t,s) \right| \le \frac{\beta}{1 - \beta N \gamma L M} \sigma(t,s) \tag{12}$$

for all $(t,s) \in [a,b] \times [a,b]$, which means that the NMPIDE (1) is Ulam–Hyers–Rassias stable.

Proof. We will study the operator $T: C^2([a,b] \times [a,b]) \to C^2([a,b] \times [a,b])$, defined by

$$(Tf)(t,s) = h(t,s) + B(t)k(\alpha(s), f(t,s))$$

$$+ \gamma k(\alpha(s), f(t,s)) \int_{a}^{s} \int_{a}^{b} \phi(\tau)G(t,\xi)\Psi(f(\xi,\tau)) d\xi d\tau$$

$$(13)$$

for all $(t, s) \in [a, b] \times [a, b]$ and $f \in C^2([a, b] \times [a, b])$.

Note that for any continuous function f, Tf is also continuous. Indeed,

$$\begin{split} \left| (Tf)(t,s) - (Tf)(t_{0},s_{0}) \right| &= \left| h(t,s) + B(t)k(\alpha(s),f(t,s)) \right| \\ &+ \gamma k(\alpha(s),f(t,s)) \int_{a}^{s} \int_{a}^{b} \phi(\tau)G(t,\xi)\Psi(f(\xi,\tau)) d\xi d\tau \\ &- h(t_{0},s_{0}) - B(t_{0})k(\alpha(s_{0}),f(t_{0},s_{0})) \\ &- \gamma k(\alpha(s_{0}),f(t_{0},s_{0})) \int_{a}^{s_{0}} \int_{a}^{b} \phi(\tau)G(t_{0},\xi)\Psi(f(\xi,\tau)) d\xi d\tau \\ &\leq \left| h(t,s) - h(t_{0},s_{0}) \right| \\ &+ \left| B(t)k(\alpha(s),f(t,s)) - B(t_{0})k(\alpha(s_{0}),f(t_{0},s_{0})) \right| \\ &+ \gamma \left| k(\alpha(s),f(t,s)) \int_{a}^{s} \int_{a}^{b} \phi(\tau)G(t,\xi)\Psi(f(\xi,\tau)) d\xi d\tau \\ &- k(\alpha(s_{0}),f(t_{0},s_{0})) \int_{a}^{s_{0}} \int_{a}^{b} \phi(\tau)G(t_{0},\xi)\Psi(f(\xi,\tau)) d\xi d\tau \\ &\leq \left| h(t,s) - h(t_{0},s_{0}) \right| + M |B(t) - B(t_{0})| \\ &+ \gamma M \left| \int_{s}^{s} \int_{a}^{b} \phi(\tau)G(t_{0},\xi)\Psi(f(\xi,\tau)) d\xi d\tau \right| \\ &\leq \left| h(t,s) - h(t_{0},s_{0}) \right| + M |B(t) - B(t_{0})| \\ &+ N\gamma M \left| \int_{s_{0}}^{s} \int_{a}^{b} \Psi(f(\xi,\tau)) d\xi d\tau \right| \to 0 \end{split}$$

when $t \to t_0$ and $s \to s_0$.

For the next phase, we will prove that the assumptions of Theorem 3.1 ensure that T is strictly contractive according to the metric specified in (4). Furthermore, for any functions f and g in $C^2([a,b] \times [a,b])$, we can derive that

$$\begin{split} d(Tf,Tg) &= \sup_{(t,s) \in [a,b] \times [a,b]} \frac{|(Tf)(t,s) - (Tg)(t,s)|}{\sigma(t,s)} \\ &= \sup_{(t,s) \in [a,b] \times [a,b]} \frac{1}{\sigma(t,s)} \left| B(t)k(\alpha(s),f(t,s)) \right. \\ &+ \gamma k(\alpha(s),f(t,s)) \int_a^s \int_a^b \phi(\tau)G(t,\xi) \Psi(f(\xi,\tau)) \, d\xi d\tau - B(t)k(\alpha(s),g(t,s)) \end{split}$$

$$\begin{split} &-\gamma k(\alpha(s),g(t,s))\int_{a}^{s}\int_{a}^{b}\phi(\tau)G(t,\xi)\Psi(g(\xi,\tau))\,d\xi d\tau \\ &\leq \gamma M\sup_{(t,s)\in[a,b]\times[a,b]}\frac{1}{\sigma(t,s)}\int_{a}^{s}\int_{a}^{b}\left|\phi(\tau)G(t,\xi)\right|\left|\Psi(f(\xi,\tau))-\Psi(g(\xi,\tau))\right|d\xi d\tau \\ &\leq N\gamma LM\sup_{(t,s)\in[a,b]\times[a,b]}\frac{1}{\sigma(t,s)}\int_{a}^{s}\int_{a}^{b}\left|f(\xi,\tau)-g(\xi,\tau)\right|d\xi d\tau \\ &=N\gamma LM\sup_{(t,s)\in[a,b]\times[a,b]}\frac{1}{\sigma(t,s)}\int_{a}^{s}\int_{a}^{b}\frac{\left|f(\xi,\tau)-g(\xi,\tau)\right|}{\sigma(\xi,\tau)}\,\sigma(\xi,\tau)\,d\xi d\tau \\ &\leq N\gamma LM\sup_{(\xi,\tau)\in[a,b]\times[a,b]}\frac{\left|f(\xi,\tau)-g(\xi,\tau)\right|}{\sigma(\xi,\tau)}\sup_{(t,s)\in[a,b]\times[a,b]}\frac{1}{\sigma(t,s)}\int_{a}^{s}\int_{a}^{b}\sigma(\xi,\tau)\,d\xi\,d\tau \\ &\leq \beta N\gamma LM\,d(f,g). \end{split}$$

Since $\beta N\gamma LM < 1$, the operator T is strictly contractive. Therefore, the Banach fixed–point theorem can be applied, ensuring that the Ulam–Hyers–Rassias stability for the NMPIDE holds.

Additionally, (12) can be derived from (3), (9) and (10). Specifically, from (9) and (10), we have:

$$|f(t,s) - (Tf)(t,s)| \le \beta \sigma(t,s), \quad (t,s) \in [a,b] \times [a,b]. \tag{14}$$

Applying the Banach fixed–point theorem once more and using (3), we obtain:

$$d(f, f_0) \le \frac{1}{1 - \beta N \gamma LM} d(Tf, f). \tag{15}$$

From the metric d and (14), it follows that:

$$\sup_{(t,s)\in[a,b]\times[a,b]} \frac{|f(t,s)-f_0(t,s)|}{\sigma(t,s)} \le \frac{\beta}{1-\beta N\gamma LM'}$$
(16)

which implies that (12) is satisfied. \Box

4. σ -semi-Ulam-Hyers Stability on a Bounded Interval

In this section, we establish new criteria for the σ -semi–Ulam–Hyers stability of the NMPIDE (1). As in Section 3, we use a nondecreasing continuous function σ , defined on $[a,b] \times [a,b]$ with values in \mathbb{R}_+ , and continue to utilize the Bielecki metric to enhance our stability analysis.

Theorem 4.1. Let $h:[a,b]\times[a,b]\to\mathbb{C}$, $B:[a,b]\to\mathbb{C}$ and $\alpha:[a,b]\to\mathbb{C}$ be continuous functions for all $(t,s)\in[a,b]\times[a,b]$ and γ be a positive constant. Assume that $k:\mathbb{C}\times\mathbb{C}\to\mathbb{C}$ is a continuous function such that there exists M>0 so that

$$M = \sup_{(t,s)\in[a,b]\times[a,b]} \left| k(\alpha(s), f(t,s)) \right|, \quad f \in \mathbb{C},$$
(17)

and $\phi:[a,b]\to\mathbb{C}$ is also continuous. Moreover, suppose that $G:[a,b]\times[a,b]\to\mathbb{C}$ represents the singular kernel of position such that there exists N>0 so that

$$\left|\phi(\tau)G(t,\xi)\right| \le N \tag{18}$$

and $\Psi: \mathbb{C} \to \mathbb{C}$ is a continuous function such that there exists L > 0 so that

$$|\Psi(f(\xi,\tau)) - \Psi(g(\xi,\tau))| \le L|f(\xi,\tau) - g(\xi,\tau)| \tag{19}$$

for all $f, g \in C^2([a, b] \times [a, b])$, and $(\xi, \tau) \in [a, b] \times [a, b]$. In addition, let $\sigma : [a, b] \times [a, b] \to \mathbb{R}_+$ be a nondecreasing continuous function such that there exists $\beta > 0$ so that

$$\int_{a}^{s} \int_{a}^{b} \sigma(\xi, \tau) \, d\xi d\tau \le \beta \sigma(t, s) \tag{20}$$

for all $(t,s) \in [a,b] \times [a,b]$.

If $f \in C^2([a,b] \times [a,b])$ is such that

$$\left| \frac{\partial}{\partial s} \left[\frac{f(t,s) - h(t,s)}{k(\alpha(s), f(t,s))} \right] - \gamma \phi(s) \int_{a}^{b} G(t,\xi) \Psi(f(\xi,s)) d\xi \right| \le \theta, \tag{21}$$

$$\left| f(t,a) - \mu(t) \right| \le \theta,\tag{22}$$

where $(t,s) \in [a,b] \times [a,b]$, $\theta \ge 0$, and $\beta N \gamma L M < 1$, then there is a unique function $f_0 \in C^2([a,b] \times [a,b])$, solution of Equation (1), that is,

$$f_0(t,s) = h(t,s) + B(t)k(\alpha(s), f_0(t,s))$$

$$+ \gamma k(\alpha(s), f_0(t,s)) \int_a^s \int_a^b \phi(\tau)G(t,\xi)\Psi(f_0(\xi,\tau)) d\xi d\tau$$
(23)

such that

$$\left| f(t,s) - f_o(t,s) \right| \le \frac{(b-a)\theta}{(1-\beta N\gamma LM)\,\sigma(a,a)} \,\sigma(t,s) \tag{24}$$

for all $(t,s) \in [a,b] \times [a,b]$, which means that the NMPIDE (1) is σ -semi–Ulam–Hyers stable.

Proof. We will study the operator $T: C^2([a,b] \times [a,b]) \to C^2([a,b] \times [a,b])$, defined by

$$(Tf)(t,s) = h(t,s) + B(t)k(\alpha(t), f(t,s))$$

$$+ \gamma k(\alpha(s), f(t,s)) \int_{a}^{s} \int_{a}^{b} \phi(\tau)G(t,\xi)\Psi(f(\xi,\tau)) d\xi d\tau$$
(25)

for all $(t, s) \in [a, b] \times [a, b]$ and $f \in C^2([a, b] \times [a, b])$ (which we have already established as well–defined). T is strictly contractive with respect to the metric defined in (4). Furthermore, for any functions f and g in $C^2([a, b] \times [a, b])$, we can derive that

$$\begin{split} d(Tf,Tg) &= \sup_{(t,s) \in [a,b] \times [a,b]} \frac{|(Tf)(t,s) - (Tg)(t,s)|}{\sigma(t,s)} \\ &= \sup_{(t,s) \in [a,b] \times [a,b]} \frac{1}{\sigma(t,s)} \left| B(t)k(\alpha(s),f(t,s)) \right. \\ &+ \gamma k(\alpha(s),f(t,s)) \int_a^s \int_a^b \phi(\tau)G(t,\xi) \Psi(f(\xi,\tau)) \, d\xi d\tau - B(t)k(\alpha(s),g(t,s)) \\ &- \gamma k(\alpha(s),g(t,s)) \int_a^s \int_a^b \phi(\tau)G(t,\xi) \Psi(g(\xi,\tau)) \, d\xi d\tau \right| \end{split}$$

$$\leq \gamma M \sup_{(t,s)\in[a,b]\times[a,b]} \frac{1}{\sigma(t,s)} \int_{a}^{s} \int_{a}^{b} \left|\phi(\tau)G(t,\xi)\right| \left|\Psi(f(\xi,\tau)) - \Psi(g(\xi,\tau))\right| d\xi d\tau$$

$$\leq N\gamma LM \sup_{(t,s)\in[a,b]\times[a,b]} \frac{1}{\sigma(t,s)} \int_{a}^{s} \int_{a}^{b} \left|f(\xi,\tau) - g(\xi,\tau)\right| d\xi d\tau$$

$$= N\gamma LM \sup_{(t,s)\in[a,b]\times[a,b]} \frac{1}{\sigma(t,s)} \int_{a}^{s} \int_{a}^{b} \frac{\left|f(\xi,\tau) - g(\xi,\tau)\right|}{\sigma(\xi,\tau)} \sigma(\xi,\tau) d\xi d\tau$$

$$\leq N\gamma LM \sup_{(\xi,\tau)\in[a,b]\times[a,b]} \frac{\left|f(\xi,\tau) - g(\xi,\tau)\right|}{\sigma(\xi,\tau)} \sup_{(t,s)\in[a,b]\times[a,b]} \frac{1}{\sigma(t,s)} \int_{a}^{s} \int_{a}^{b} \sigma(\xi,\tau) d\xi d\tau$$

$$\leq \beta N\gamma LM d(f,g).$$

Since $\beta N\gamma LM$ < 1, the operator T is strictly contractive. Therefore, the Banach fixed–point theorem can be applied, ensuring that the σ –semi–Ulam–Hyers stability for the NMPIDE (1) holds.

On the other hand, considering (21), (22) and the definition of T, it follows that

$$|f(t,s) - (Tf)(t,s)| \le (b-a)\theta, \quad (t,s) \in [a,b] \times [a,b].$$
 (26)

Furthermore, by applying (3), the definition of the metric *d*, and using (26), we obtain

$$\sup_{(t,s)\in[a,b]\times[a,b]} \frac{|f(t,s) - f_0(t,s)|}{\sigma(t,s)} \le \frac{1}{1 - \beta N \gamma L M} \sup_{(t,s)\in[a,b]\times[a,b]} \frac{(b-a)\theta}{\sigma(t,s)},\tag{27}$$

which, by the definition of σ , implies that (24) holds. \square

5. Ulam-Hyers Stability on a Bounded Interval

In this section, we establish new criteria for the Ulam–Hyers stability of the NMPIDE (1). As in results obtained earlier, we use a nondecreasing continuous function σ , defined on $[a,b] \times [a,b]$ with values in \mathbb{R}_+ , and continue to utilize the Bielecki metric (4) to enhance our stability analysis.

Theorem 5.1. Let $h:[a,b]\times[a,b]\to\mathbb{C}$, $B:[a,b]\to\mathbb{C}$ and $\alpha:[a,b]\to\mathbb{C}$ be continuous functions for all $(t,s)\in[a,b]\times[a,b]$ and γ be a positive constant. Assume that $k:\mathbb{C}\times\mathbb{C}\to\mathbb{C}$ is a continuous function such that there exists M>0 so that

$$M = \sup_{(t,s)\in[a,b]\times[a,b]} \left| k(\alpha(s), f(t,s)) \right|, \quad f \in \mathbb{C},$$
(28)

and $\phi:[a,b]\to\mathbb{C}$ is also continuous. Moreover, suppose that $G:[a,b]\times[a,b]\to\mathbb{C}$ represents the singular kernel of position such that there exists N>0 so that

$$\left|\phi(\tau)G(t,\xi)\right| \le N \tag{29}$$

and $\Psi: \mathbb{C} \to \mathbb{C}$ is a continuous function such that there exists L > 0 so that

$$|\Psi(f(\xi,\tau)) - \Psi(g(\xi,\tau))| \le L|f(\xi,\tau) - g(\xi,\tau)| \tag{30}$$

for all $f, g \in C^2([a,b] \times [a,b])$ and $(\xi, \tau) \in [a,b] \times [a,b]$. In addition, let $\sigma : [a,b] \times [a,b] \to \mathbb{R}_+$ be a nondecreasing continuous function such that there exists $\beta > 0$ so that

$$\int_{a}^{s} \int_{a}^{b} \sigma(\xi, \tau) d\xi d\tau \le \beta \sigma(t, s) \tag{31}$$

for all $(t,s) \in [a,b] \times [a,b]$.

If $f \in C^2([a,b] \times [a,b])$ is such that

$$\left| \frac{\partial}{\partial s} \left[\frac{f(t,s) - h(t,s)}{k(\alpha(s), f(t,s))} \right] - \gamma \phi(s) \int_{a}^{b} G(t,\xi) \Psi(f(\xi,s)) d\xi \right| \le \theta, \tag{32}$$

$$\left| f(t,a) - \mu(t) \right| \le \theta,\tag{33}$$

where $(t,s) \in [a,b] \times [a,b]$, $\theta \ge 0$, and $\beta N \gamma L M < 1$, then there is a unique function $f_0 \in C^2([a,b] \times [a,b])$, solution of Equation (1), that is,

$$f_0(t,s) = h(t,s) + B(t)k(\alpha(s), f_0(t,s))$$

$$+ \gamma k(\alpha(s), f_0(t,s)) \int_a^s \int_a^b \phi(\tau)G(t,\xi)\Psi(f_0(\xi,\tau)) d\xi d\tau$$
(34)

such that

$$\left| f(t,s) - f_o(t,s) \right| \le \frac{(b-a)\sigma(b,b)}{(1-\beta N\gamma LM)\,\sigma(a,a)}\,\theta \tag{35}$$

for all $(t,s) \in [a,b] \times [a,b]$, which means that the NMPIDE (1) is Ulam–Hyers stable.

Proof. By applying a similar argument as above, the Banach fixed–point theorem from this study ensures the Ulam–Hyers stability for the NMPIDE (1). Since $\beta N\gamma LM < 1$, the results obtained earlier confirm that T is strictly contractive, thereby validating the approach used in Theorem 5.1. \square

6. Ulam-Hyers-Rassias Stability on an Unbounded Interval

In this section, we will explore the Ulam–Hyers–Rassias stability of the NMPIDE (1) over unbounded intervals. Unlike the previous analysis on bounded Intervals $[a,b] \times [a,b]$ (where $a,b \in \mathbb{R}$), we will now shift our focus to intervals of the form $[a,\infty) \times [a,\infty)$, with a as a fixed real number.

Thus, we will now consider the NMPIDE with discontinuous kernel,

$$\frac{\partial}{\partial s} \left[\frac{f(t,s) - h(t,s)}{k(\alpha(s), f(t,s))} \right] = \gamma \phi(s) \int_{a}^{\infty} G(t,\xi) \Psi(f(\xi,s)) d\xi,$$

$$f(t,a) = \mu(t),$$
(36)

with $(t,s) \in [a,\infty) \times [a,\infty)$, where, a is a fixed real number, $h:[a,\infty) \times [a,\infty) \to \mathbb{C}$, $\alpha:[a,\infty) \to \mathbb{C}$, $k:\mathbb{C} \times \mathbb{C} \to \mathbb{C}$, $\phi:[a,\infty) \to \mathbb{C}$, $\Psi:\mathbb{C} \to \mathbb{C}$ are bounded continuous functions, $G:[a,\infty) \times [a,\infty) \to \mathbb{C}$ represents the singular kernel of position, $f \in C^2([a,\infty) \times [a,\infty))$, γ is a constant, and $\mu:[a,\infty) \to \mathbb{C}$ is the initial function.

It is straightforward to demonstrate that Equation (36) is equivalent to the integral equation

$$f(t,s) = h(t,s) + B(t)k(\alpha(s), f(t,s)) + \gamma k(\alpha(s), f(t,s)) \int_{a}^{s} \int_{a}^{\infty} \phi(\tau)G(t,\xi)\Psi(f(\xi,\tau)) d\xi d\tau,$$
(37)

where

$$B(t) = \left[\frac{(\mu(t) - h(t, a))}{k(\alpha(a), \mu(t))}\right].$$

In this case, we will apply a recurrence method, making use of the results obtained earlier for the associated bounded interval.

Let us consider a fixed, nondecreasing, continuous function $\sigma: [a, \infty) \times [a, \infty) \to (\varepsilon, \omega)$, where $\varepsilon, \omega > 0$, and consider the space $C_h^2([a, \infty) \times [a, \infty))$ of bounded functions, equipped with the metric [22]

$$d_b(f,g) = \sup_{\substack{(t,s) \in [a,\infty) \times [a,\infty) \\ \sigma(t,s)}} \frac{|f(t,s) - g(t,s)|}{\sigma(t,s)}.$$
(38)

Theorem 6.1. Let $h:[a,\infty)\times[a,\infty)\to\mathbb{C}$, $B:[a,\infty)\to\mathbb{C}$ and $\alpha:[a,\infty)\to\mathbb{C}$ be bounded continuous functions for all $(t,s)\in[a,\infty)\times[a,\infty)$ and γ be a positive constant. Assume that $k:\mathbb{C}\times\mathbb{C}\to\mathbb{C}$ is a bounded continuous function such that there exists M>0 so that

$$M = \sup_{(t,s)\in[a,\infty)\times[a,\infty)} \left| k(\alpha(s), f(t,s)) \right|, \quad f \in \mathbb{C},$$
(39)

and $\phi:[a,\infty)\to\mathbb{C}$ is also a bounded continuous function. Moreover, suppose that $G:[a,\infty)\times[a,\infty)\to\mathbb{C}$ represents the singular kernel of position such that there exists N>0 so that

$$\left|\phi(\tau)G(t,\xi)\right| \le N\tag{40}$$

and $\Psi: \mathbb{C} \to \mathbb{C}$ is a bounded continuous function such that there exists L > 0 so that

$$|\Psi(f(\xi,\tau)) - \Psi(g(\xi,\tau))| \le L|f(\xi,\tau) - g(\xi,\tau)| \tag{41}$$

for all $f,g \in C_b^2([a,\infty) \times [a,\infty))$, and $(\xi,\tau) \in [a,\infty) \times [a,\infty)$. In addition, let $\sigma:[a,\infty) \times [a,\infty) \to \mathbb{R}_+$ be a nondecreasing continuous function such that there exists $\beta > 0$ so that

$$\int_{a}^{s} \int_{a}^{\infty} \sigma(\xi, \tau) \, d\xi d\tau \le \beta \sigma(t, s) \tag{42}$$

for all $(t,s) \in [a,\infty) \times [a,\infty)$.

If $f \in C_b^2([a,\infty) \times [a,\infty))$ is such that

$$\left| \frac{\partial}{\partial s} \left[\frac{f(t,s) - h(t,s)}{k(\alpha(s), f(t,s))} \right] - \gamma \phi(s) \int_{a}^{\infty} G(t,\xi) \Psi(f(\xi,s)) d\xi \right| \le \sigma(t,s), \tag{43}$$

$$\left| f(t,a) - \mu(t) \right| \le \sigma(t,s),\tag{44}$$

where $(t,s) \in [a,\infty) \times [a,\infty)$, and $\beta N \gamma L M < 1$, then there is a unique function $f_0 \in C_b^2([a,\infty) \times [a,\infty))$, solution of Equation (36), that is,

$$f_0(t,s) = h(t,s) + B(t)k(\alpha(s), f_0(t,s))$$

$$+ \gamma k(\alpha(s), f_0(t,s)) \int_s^s \int_s^\infty \phi(\tau)G(t,\xi)\Psi(f_0(\xi,\tau)) d\xi d\tau$$

$$(45)$$

such that

$$\left| f(t,s) - f_o(t,s) \right| \le \frac{\beta}{1 - \beta N \gamma L M} \, \sigma(t,s) \tag{46}$$

for all $(t,s) \in [a,\infty) \times [a,\infty)$, which means that the NMPIDE (36) is Ulam–Hyers–Rassias stable.

Proof. For any $n \in \mathbb{N}$, we define $I_n = [a, a + n]$. According to Theorem 3.1, there exists a unique continuous function $f_{0,n} \in C^2(I_n \times I_n)$ that satisfies

$$f_{0,n}(t,s) = h(t,s) + B(t)k(\alpha(s), f_{0,n}(t,s)) + \gamma k(\alpha(s), f_{0,n}(t,s)) \int_{a}^{s} \int_{a}^{a+n} \phi(\tau)G(t,\xi)\Psi(f_{0,n}(\xi,\tau)) d\xi d\tau.$$
(47)

Moreover, the function satisfies the inequality

$$\left| f(t,s) - f_{0,n}(t,s) \right| \le \frac{\beta}{1 - \beta N \gamma L M} \, \sigma(t,s) \tag{48}$$

for all $(t,s) \in I_n \times I_n$. The uniqueness of $f_{0,n}$ implies that if $(t,s) \in I_n \times I_n$, then

$$f_{0,n}(t,s) = f_{0,n+1}(t,s) = f_{0,n+2}(t,s) = \cdots$$
 (49)

For any $(t,s) \in [a,\infty) \times [a,\infty)$, we define $n(t,s) \in \mathbb{N}$ as

$$n(t,s) = \min\{n \in \mathbb{N} \mid (t,s) \in I_n \times I_n\}.$$

Additionally, we define the function $f_0: [a, \infty) \times [a, \infty) \to \mathbb{C}$ by

$$f_0(t,s) = f_{0,n(t,s)}(t,s).$$
 (50)

For any $(t_1, s_1) \in [a, \infty) \times [a, \infty)$, let $n_1 = n(t_1, s_1)$. Then, we have $(t_1, s_1) \in Int(I_{n_1+1} \times I_{n_1+1})$, meaning there exists $\epsilon > 0$ such that $f_0(t, s) = f_{0,n_1+1}(t, s)$ for all $(t, s) \in ((t_1, s_1) - \epsilon, (t_1, s_1) + \epsilon) \times ((t_1, s_1) - \epsilon, (t_1, s_1) + \epsilon)$. Here, $Int(I_{n_1+1} \times I_{n_1+1})$ denotes the interior of the set $I_{n_1+1} \times I_{n_1+1}$. By Theorem 3.1, the function f_{0,n_1+1} is continuous at (t_1, s_1) , which implies that f_0 is also continuous.

Next, we show that f_0 satisfies

$$f_0(t,s) = h(t,s) + B(t)k(\alpha(s), f_0(t,s))$$

$$+ \gamma k(\alpha(s), f_0(t,s)) \int_a^s \int_a^\infty \phi(\tau)G(t,\xi)\Psi(f_0(\xi,\tau)) d\xi d\tau,$$
(51)

as well as the inequality

$$\left| f(t,s) - f_o(t,s) \right| \le \frac{\beta}{1 - \beta N \gamma L M} \, \sigma(t,s). \tag{52}$$

For an arbitrary $(t,s) \in [a,\infty) \times [a,\infty)$, we select n(t,s) such that $(t,s) \in I_{n(t,s)} \times I_{n(t,s)}$. Using (47) and (50), we obtain

$$f_{0}(t,s) = f_{0,n(t,s)}(t,s)$$

$$= h(t,s) + B(t)k(\alpha(s), f_{0,n(t,s)}(t,s))$$

$$+ \gamma k(\alpha(s), f_{0,n(t,s)}(t,s)) \int_{a}^{s} \int_{a}^{a+n(t,s)} \phi(\tau)G(t,\xi)\Psi(f_{0,n(t,s)}(\xi,\tau)) d\xi d\tau$$

$$= h(t,s) + B(t)k(\alpha(s), f_{0}(t,s))$$

$$+ \gamma k(\alpha(s), f_{0}(t,s)) \int_{a}^{s} \int_{a}^{\infty} \phi(\tau)G(t,\xi)\Psi(f_{0}(\xi,\tau)) d\xi d\tau.$$
(53)

Noting that $n(\rho, \nu) \le n(t, s)$ for any $(\rho, \nu) \in I_{n(t, s)} \times I_{n(t, s)}$, it follows from (49) that $f_0(\rho, \nu) = f_{0, n(\rho, \nu)}(\rho, \nu) = f_{0, n(t, s)}(\rho, \nu)$, thus confirming the final equality in (53).

To establish (46), we use (50) and (48), yielding

$$\left| f(t,s) - f_0(t,s) \right| = \left| f(t,s) - f_{0,n(t,s)}(t,s) \right| \le \frac{\beta}{1 - \beta N \gamma L M} \sigma(t,s), \tag{54}$$

for all $(t,s) \in [a,\infty) \times [a,\infty)$.

Finally, we prove the uniqueness of f_0 . Suppose that another bounded continuous function f_1 satisfies (45) and (46) for all $(t,s) \in [a,\infty) \times [a,\infty)$. By the uniqueness of the solution on $I_{n(t,s)}$ for any $n(t,s) \in \mathbb{N}$, it follows that $f_{0|I_{n(t,s)} \times I_{n(t,s)}} = f_{0,n(t,s)}$ and $f_{1|I_{n(t,s)} \times I_{n(t,s)}}$ satisfies (45) and (46) for all $(t,s) \in I_{n(t,s)} \times I_{n(t,s)}$. Consequently, we conclude that

$$f_0(t,s) = f_0 \mid_{I_{n(t,s)} \times I_{n(t,s)}} (t,s) = f_1 \mid_{I_{n(t,s)} \times I_{n(t,s)}} (t,s) = f_1(t,s).$$

7. Illustrative Examples

In this section, we will provide four examples to demonstrate that the conditions established in the above results can indeed be satisfied.

Example 7.1. Consider the following NMPIDE with the condition:

$$\begin{cases} \frac{\partial}{\partial s} \left[\frac{f(t,s) - e^{-s}t(s+2) \left(\frac{1}{400} \left(\frac{1}{|t-1|} - \frac{1}{2|t-1|^2} - \frac{1}{|t|} \right) \left(\frac{s^3}{3} + s^2 \right) + e^s - 1 \right)}{e^{-s}f(t,s)} \right] \\ = \frac{s}{4} \int_0^1 \frac{|t-\xi|^{-3}}{100} f(\xi,s) \, d\xi, \\ f(t,0) = \frac{99}{50} t, \end{cases}$$
(55)

with $(t,s) \in [0,1] \times [0,1]$.

We confirm that all the conditions of Theorem 3.1 are fulfilled. The exact solution of the equation is known to be $f_0(t,s) = t(s+2)$.

By comparing Equations (1) and (55) and performing some related mathematical computations, we obtain the following estimates:

$$\begin{split} [a,b] &= [0,1], \gamma = \frac{1}{4}, \quad (t,s), (\xi,\tau) \in [0,1] \times [0,1]; \\ h(t,s) &= e^{-s}t(s+2) \left[\frac{1}{400} \left(\frac{1}{|t-1|} - \frac{1}{2|t-1|^2} - \frac{1}{|t|} \right) \left(\frac{s^3}{3} + s^2 \right) + e^s - 1 \right], \\ k(\alpha(s), f(t,s)) &= e^{-s}f(t,s), \\ \sup_{(t,s) \in [a,b] \times [a,b]} \left| k(\alpha(s), f(t,s)) \right| &= \sup_{(t,s) \in [0,1] \times [0,1]} \left| e^{-s}f(t,s) \right| \leq 3 = M; \\ \phi(s) &= s, \quad G(t,\xi) = \frac{1}{100} \left| t - \xi \right|^{-3}, \\ \left| \phi(\tau)G(t,\xi) \right| &= \frac{1}{100} \left| \tau \left| t - \xi \right|^{-3} \right| \leq \frac{1}{100} = N; \\ \mu(t) &= \frac{99}{50}t, \quad \Psi(f(\xi,\tau)) = f(\xi,\tau), \end{split}$$

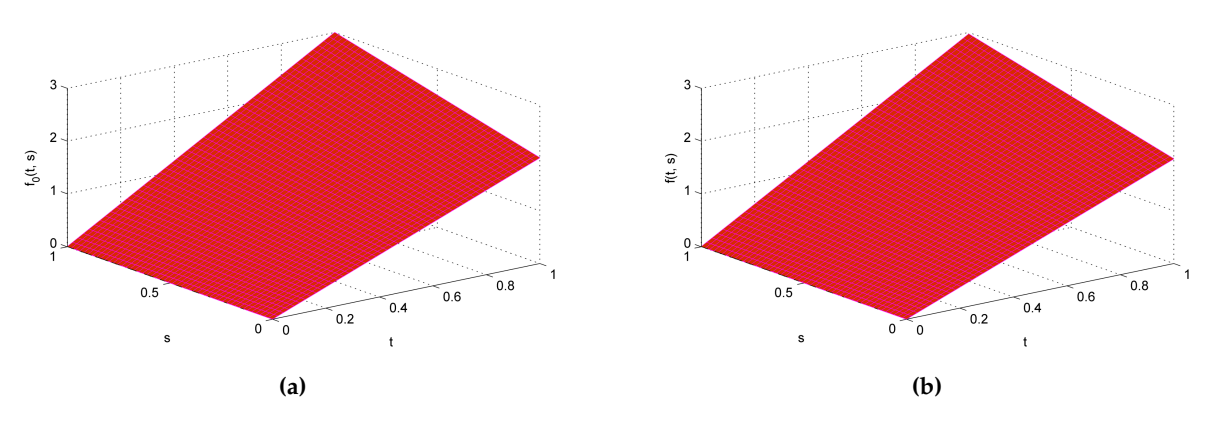


Figure 1: The first graph depicts the exact solution f_0 , while the second graph illustrates the approximate solution f for Equation (55) over the interval $(t,s) \in [0,1] \times [0,1]$. The exact solution represents the ideal mathematical model, whereas the approximate solution provides a closely matching estimate with slight deviations. The comparison reveals that the approximate solution remains consistently bounded by the exact solution, ensuring the Ulam–Hyers–Rassias stability of the system. This bounded behavior signifies that any deviations in the approximate solution do not grow unbounded but remain well-controlled, reinforcing the accuracy and reliability of the approximation in capturing the system's dynamics.

$$\begin{split} \left| \Psi(f(\xi, \tau)) - \Psi(g(\xi, \tau)) \right| \\ &= \left| f(\xi, \tau) - g(\xi, \tau) \right| \\ &\leq \frac{11}{10} \left| f(\xi, \tau) - g(\xi, \tau) \right| \\ &= L \left| f(\xi, \tau) - g(\xi, \tau) \right|, \ \forall \ f, g \in C^2 \left([0, 1] \times [0, 1] \right). \end{split}$$

Moreover, we assume that there is $\beta > 0$ *, such that*

$$\int_0^s \int_0^1 \sigma(\xi, \tau) \, d\xi d\tau = \int_0^s \int_0^1 5e^{\xi + \tau} \, d\xi d\tau \le 5(e - 1)e^{t + s} = \beta \sigma(t, s),$$

where $\sigma(t,s) = 5e^{t+s}$ is the nondecreasing continuous function. Using MATLAB, the exact solution f_0 and the approximate solution f_0 of Equation (55) are illustrated in Fig. 1 and Fig. 2.

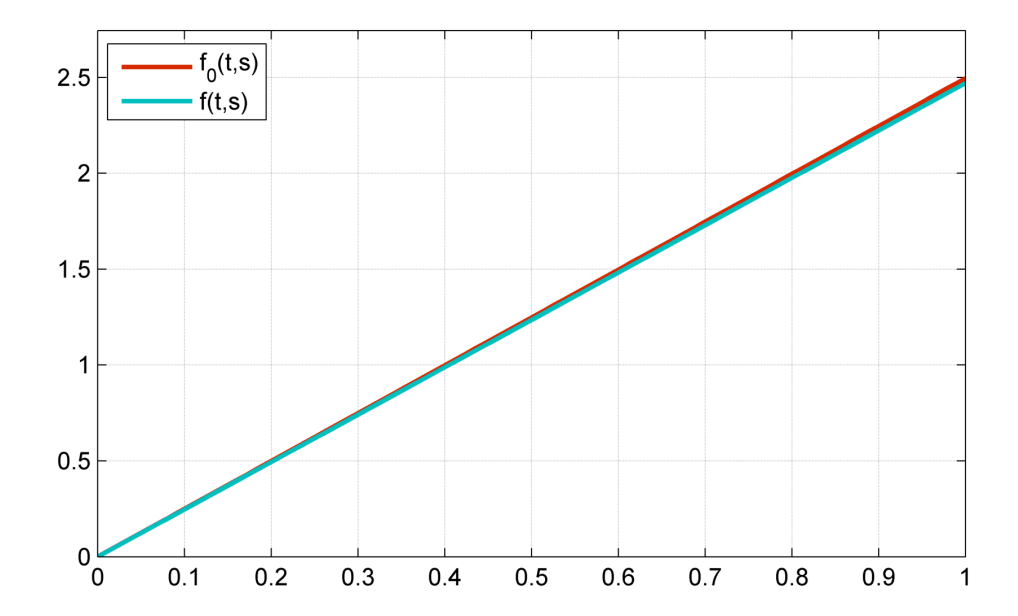


Figure 2: 2D plot comparing the exact solution $f_0(t,s)$ and the approximate solution f(t,s) for Equation (55) over the interval $[0,1] \times [0,1]$. The exact solution represents the ideal mathematical model, while the approximate solution provides a closely matching estimate with slight deviations. The comparison underscores the bounded nature of the approximate solution relative to the exact solution, ensuring Ulam–Hyers–Rassias stability. This bounded behavior guarantees that any deviations in the approximate solution remain controlled, reinforcing the reliability of the approximation in capturing the system's dynamics.

If we choose $f(t,s) = \frac{99}{100}t(s+2)$, it follows,

$$\left| \frac{\partial}{\partial s} \left[\frac{f(t,s) - h(t,s)}{k(\alpha(s), f(t,s))} \right] - \gamma \phi(s) \int_{0}^{1} G(t,\xi) \Psi(f(\xi,s)) d\xi \right|
= \left| \frac{e^{s}}{99} + \frac{s(s+2)}{5000} \left(\frac{19}{|t-1|} - \frac{13}{2|t|} \right) \right| \le 5e^{t+s} = \sigma(t,s),$$
(56)

$$|f(t,0) - \mu(t)| = 0 \le 5e^{t+s} = \sigma(t,s),$$
 (57)

where $(t,s) \in [0,1] \times [0,1]$. Fig. 3 represents the graphs of the functions appearing in (56) and (57).

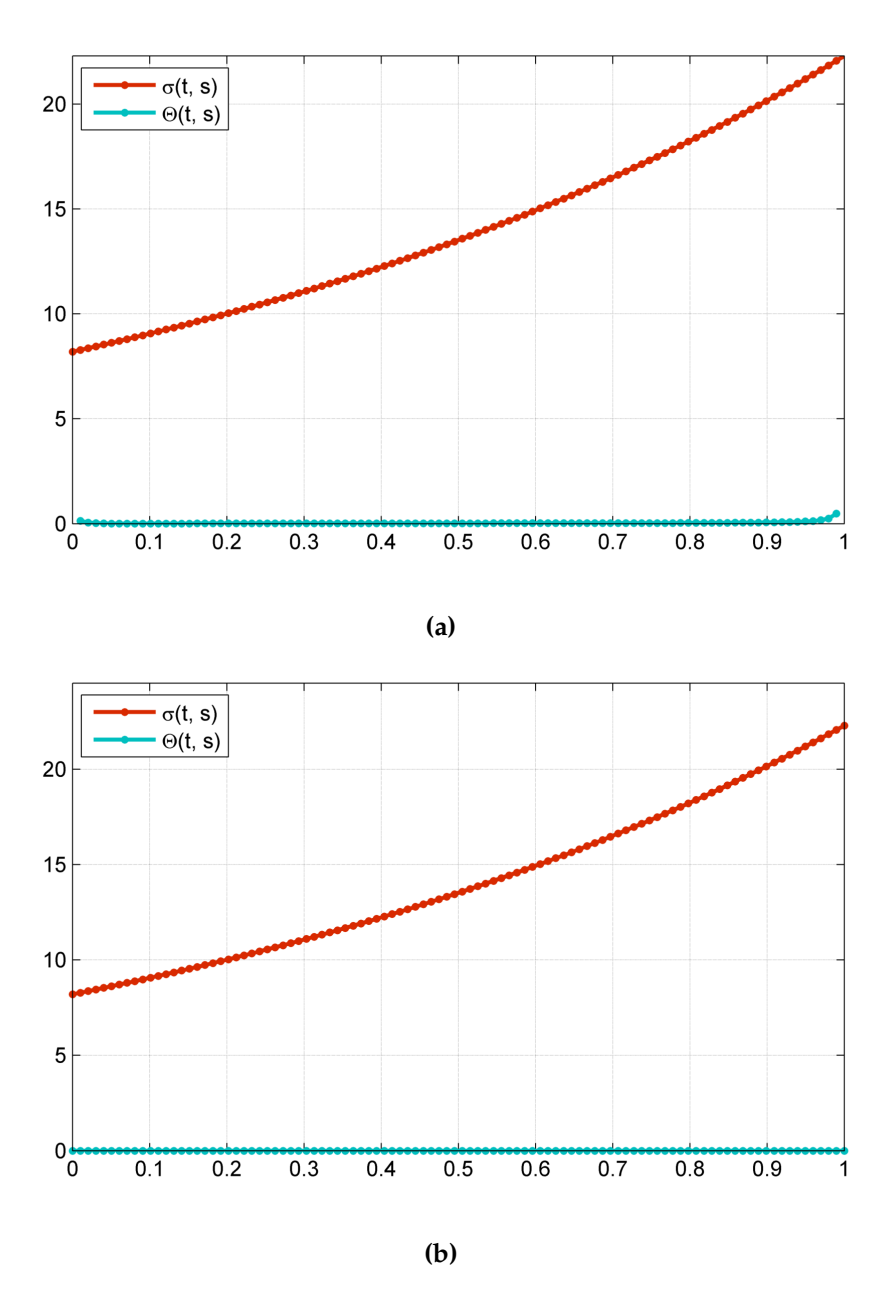


Figure 3: (a) 2D plot of the inequality (56), comparing the two functions: $\Theta(t,s) = \left| \frac{e^s}{99} + \frac{s(s+2)}{5000} \left(\frac{19}{|t-1|} - \frac{13}{2|t|} \right) \right|$, denoted by a blue line, and $\sigma(t,s) = 5e^{t+s}$, denoted by a red line. **(b)** 2D plot of the inequality (57), comparing the functions: $\Theta(t,s) = 0$, denoted by a blue line, and $\sigma(t,s) = 5e^{t+s}$, denoted by a red line; These plots illustrate the bounded relationship between $\Theta(t,s)$ and $\sigma(t,s)$, demonstrating that deviations remain within a prescribed bound. This bounded behavior ensures Ulam–Hyers–Rassias stability, highlighting the system's resistance to perturbations. By visualizing these variations, the plots provide a clear representation of stability constraints, reinforcing the robustness of the system under small deviations.

This demonstrates the Ulam–Hyers–Rassias stability of the Equation (55). Furthermore, considering the exact solution $f_0(t,s) = t(s+2)$ and the fact that $\beta N \gamma L M = 0.01417582508 < 1$, we have

$$\left| f(t,s) - f_0(t,s) \right| = \left| \frac{99}{100} t(s+2) - t(s+2) \right|$$

$$\leq \frac{4000(e-1)}{4000 - 33(e-1)} 5e^{t+s}$$

$$= \frac{\beta}{1 - \beta N \gamma LM} \sigma(t,s), \quad (t,s) \in [0,1] \times [0,1];$$
(58)

see Fig. 4.

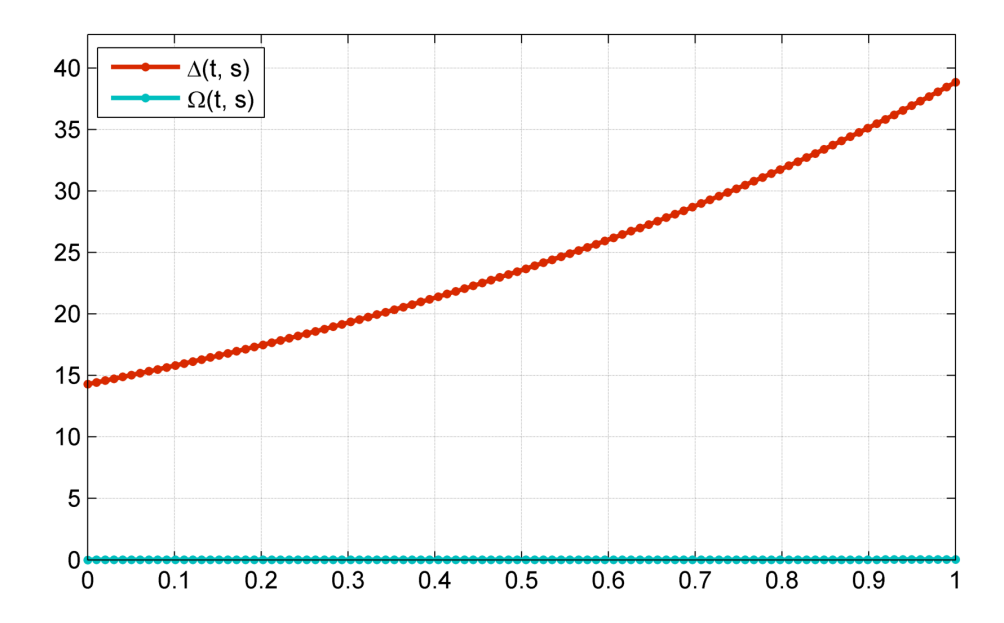


Figure 4: 2D plot of the inequality (58) illustrating a comparison between the two functions: $\Omega(t,s) = \left|\frac{99}{100}t(s+2) - t(s+2)\right|$, denoted by a blue line, and $\Delta(t,s) = \frac{\beta}{1-\beta N\gamma LM}\sigma(t,s) = \frac{4000(e-1)}{4000-33(e-1)}$ 5 e^{t+s} , denoted by a red line. This plot highlights the relationship between $\Omega(t,s)$ and $\Delta(t,s)$, demonstrating that $\Omega(t,s)$ remains bounded within $\Delta(t,s)$. This bounded behavior is crucial in Ulam–Hyers–Rassias stability analysis, ensuring that perturbations in the system remain controlled within a predefined limit. The comparison provides valuable insight into the stability properties of the system, reinforcing the reliability of the approximate model in capturing controlled variations over the given interval.

Example 7.2. Consider the following NMPIDE with the condition:

$$\begin{cases} \frac{\partial}{\partial s} \left[\frac{f(t,s) + \frac{\sin(s)}{77} \left(s + 71(s+1) \left(\frac{1}{15400000} \ln \left| \frac{t-1}{t} \left| \cos(2s) - 1 \right) \right) \right)}{(s+1)f(t,s)} \right] \\ = 71 \cos(s) \int_{0}^{1} \frac{1}{50|t-\xi|} \frac{f(\xi,s)}{1000} d\xi, \\ f(t,0) = 0, \end{cases}$$
(59)

with $(t,s) \in [0,1] \times [0,1]$.

We confirm that all the conditions of Theorem 4.1 are fulfilled. The exact solution of the equation is known to be $f_0(t,s) = \frac{\sin(s)}{77}$.

By comparing Equations (1) and (59) and performing some related mathematical computations, we obtain the following estimates:

$$[a,b] = [0,1], \gamma = 71, \quad (t,s), (\xi,\tau) \in [0,1] \times [0,1];$$

$$h(t,s) = -\frac{\sin(s)}{77} \left[s + 71(s+1) \left(\frac{\ln\left|\frac{t-1}{t}\right|}{15400000} (\cos(2s) - 1) \right) \right],$$

$$k(\alpha(s), f(t,s)) = (s+1)f(t,s),$$

$$\sup_{(t,s)\in[a,b]\times[a,b]} \left| k(\alpha(s), f(t,s)) \right| = \sup_{(t,s)\in[0,1]\times[0,1]} \left| (s+1)f(t,s) \right| \le 2 = M;$$

$$\phi(s) = \cos(s), \quad G(t,\xi) = \frac{1}{50|t-\xi|},$$

$$\left| \phi(\tau)G(t,\xi) \right| = \frac{1}{50} \left| \frac{\cos(\tau)}{t-\xi} \right| \le \frac{1}{50} = N;$$

$$\mu(t) = 0, \quad \Psi(f(\xi,\tau)) = \frac{1}{1000} f(\xi,\tau),$$

$$\left| \Psi(f(\xi,\tau)) - \Psi(g(\xi,\tau)) \right|$$

$$= \left| \frac{1}{1000} f(\xi,\tau) - \frac{1}{1000} g(\xi,\tau) \right|$$

$$\le \frac{1}{100} \left| f(\xi,\tau) - g(\xi,\tau) \right|, \quad \forall f,g \in C^2([0,1] \times [0,1]).$$

Moreover, we assume that there is $\beta > 0$, such that

$$\int_{0}^{s} \int_{0}^{1} \sigma(\xi, \tau) \, d\xi d\tau = \int_{0}^{s} \int_{0}^{1} e^{3\xi + 2\tau} \, d\xi d\tau \le (e^{3} - 1)e^{3t + 2s} = \beta \sigma(t, s),$$

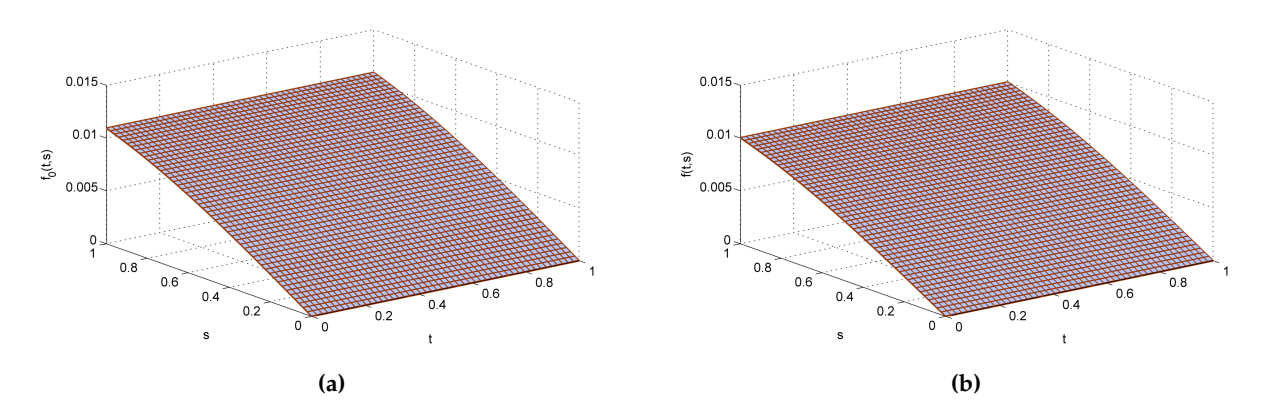


Figure 5: These 3D plots depict the exact solution f_0 and the approximate solution f for Equation (59), both visualized over the interval $[0,1] \times [0,1]$. The comparison provides a detailed examination of the σ -semi–Ulam–Hyers stability properties of f in relation to f_0 , highlighting the extent of deviation and the rate of convergence across the specified domain. The visualizations serve to assess the boundedness and structural consistency of f under perturbations, ensuring that any deviations remain controlled within the stability framework. This analysis reinforces the reliability and accuracy of the approximation, demonstrating that the approximate solution adheres to the prescribed stability constraints.

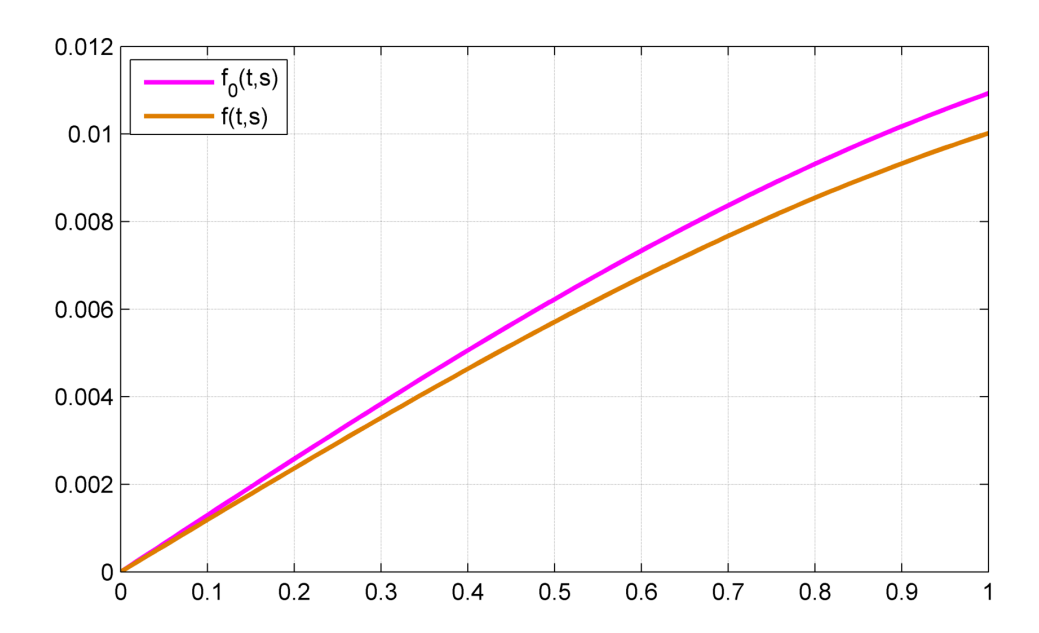


Figure 6: This 2D plot presents the exact solution $f_0(t,s)$ and the approximate solution f(t,s) for Equation (59), both defined over the domain $[0,1] \times [0,1]$. The visualization provides a detailed comparison of their behavior with respect to both t and s, offering insights into the σ -semi–Ulam–Hyers stability and accuracy of the approximation. The graphical representation highlights the extent of deviation between f_0 and f, allowing for an assessment of the convergence properties and the reliability of the approximation across the specified interval.

where $\sigma(t,s)=e^{3t+2s}$ is the nondecreasing continuous function. Using MATLAB, the exact solution f_0 and the approximate solution f of Equation (59) are illustrated in Fig. 5 and Fig. 6. If we choose $f(t,s) = \frac{\sin(s)}{84}$, it follows,

$$\left| \frac{\partial}{\partial s} \left[\frac{f(t,s) - h(t,s)}{k(\alpha(s), f(t,s))} \right] - \gamma \phi(s) \int_0^1 G(t,\xi) \Psi(f(\xi,s)) d\xi \right|$$

$$= \left| \frac{1}{11(s+1)^2} \right| \le \frac{350000}{13750} = \theta,$$
(60)

$$\left| f(t,0) - \mu(t) \right| = 0 \le \frac{350000}{13750} = \theta,\tag{61}$$

where $(t,s) \in [0,1] \times [0,1]$. Fig. 7 represents the graphs of the functions appearing in (60) and (61).

This demonstrates the σ–semi–Ulam–Hyers stability of the Equation (59). Furthermore, considering the exact solution $f_0(t,s) = \frac{\sin(s)}{77}$ and the fact that $\beta N \gamma LM = 0.5420292486 < 1$, we have

$$\left| f(t,s) - f_0(t,s) \right| = \left| \frac{\sin(s)}{84} - \frac{\sin(s)}{77} \right|$$

$$\leq \frac{350000}{13750 \left[1 - \left(\frac{e^3 - 1}{50} \right) \left(\frac{71}{50} \right) \right]} e^{3t + 2s}$$

$$= \frac{(b - a)\theta}{(1 - \beta N \gamma LM) \sigma(0,0)} \sigma(t,s), \quad (t,s) \in [0,1] \times [0,1];$$
(62)

see Fig. 8.

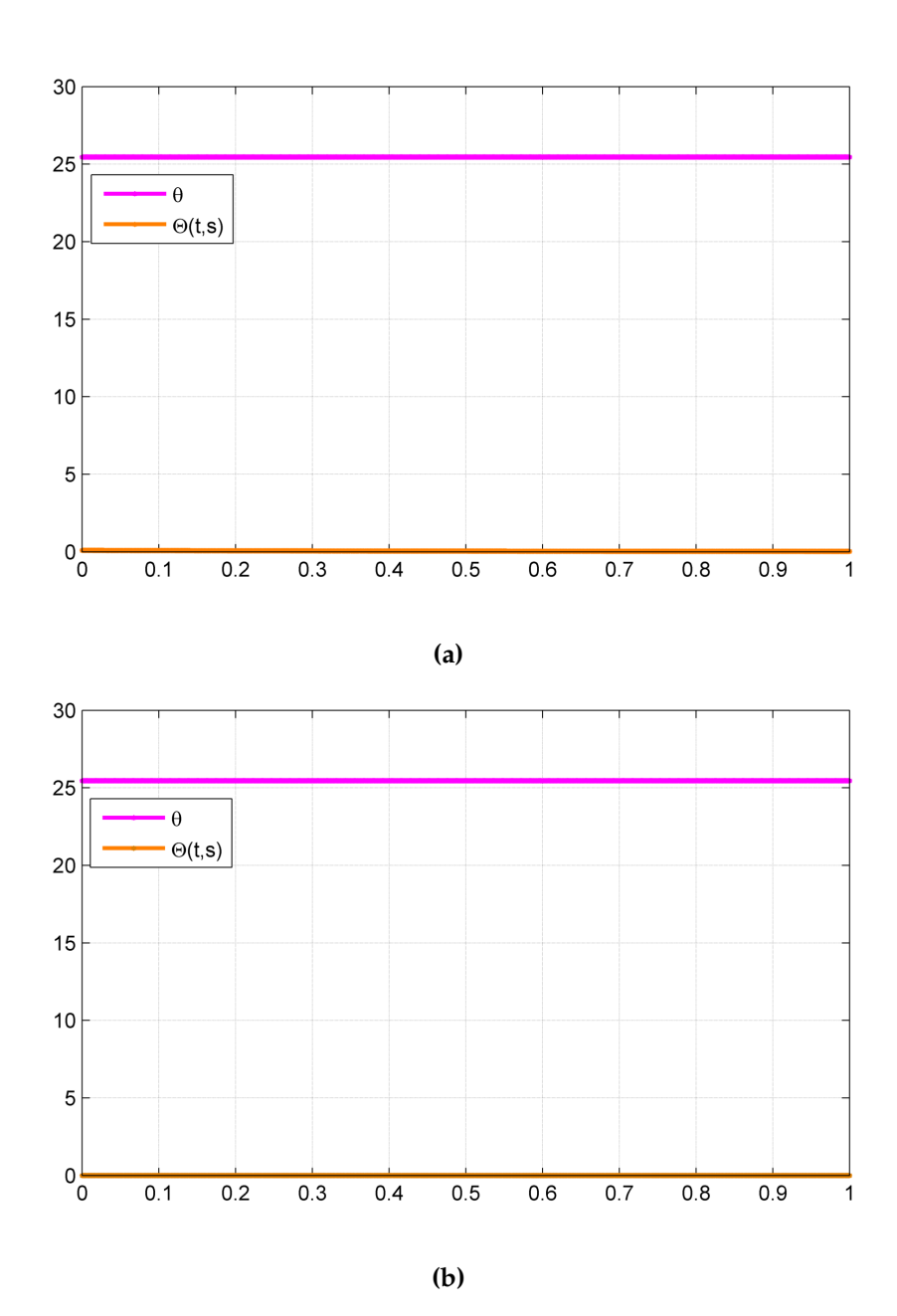


Figure 7: (a) 2D plot of the inequality (60), illustrating the stability–bound comparison between the functions: $\Theta(t,s) = \left|\frac{1}{11(s+1)^2}\right|$, denoted by an orange line, and $\theta = \frac{350000}{13750}$, denoted by a pink line. This visualization examines the boundedness of $\Theta(t,s)$ within the specified domain, offering insights into the constraints necessary for ensuring σ–semi–Ulam–Hyers stability; (b) 2D plot of the inequality (61), comparing $\Theta(t,s) = 0$, denoted by an orange line, and $\theta = \frac{350000}{13750}$, denoted by a pink line. This figure highlights the limiting case where deviations are controlled within a prescribed bound, reinforcing the concept of σ–semi–Ulam–Hyers stability by ensuring that perturbations in the system remain constrained and well–regulated under the given stability framework.

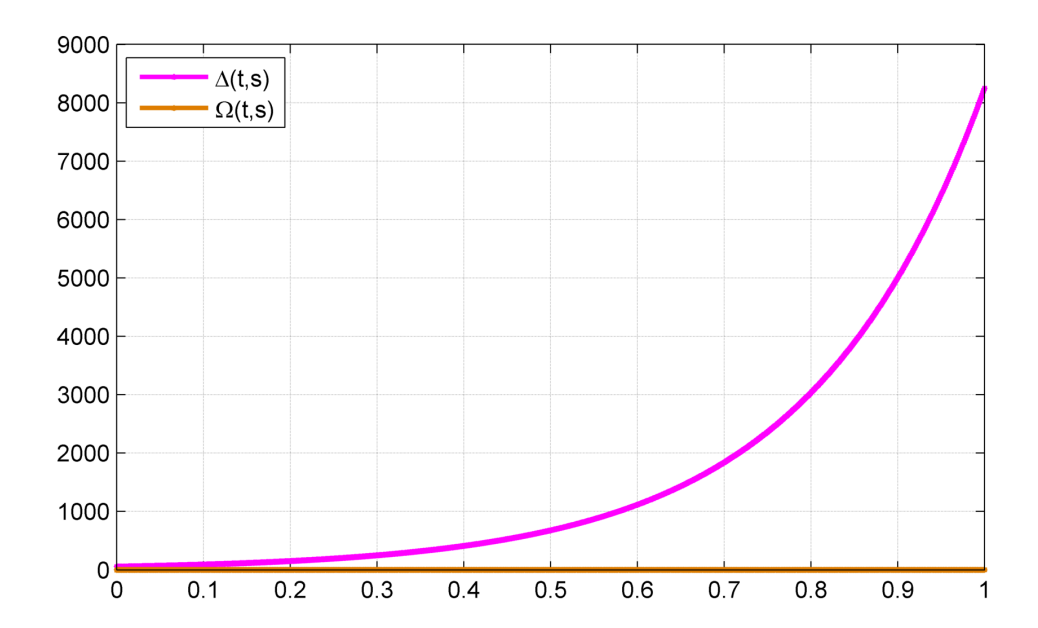


Figure 8: 2D plot of the inequality (62), illustrating the stability–bound comparison between the functions: $\Omega(t,s) = \left|\frac{\sin(s)}{84} - \frac{\sin(s)}{77}\right|$, represented by an orange line, and $\Delta(t,s) = \frac{(b-a)\theta}{(1-\beta N\gamma LM)\sigma(0,0)}\sigma(t,s) = \frac{350000}{13750\left[1-\left(\frac{c^3-1}{50}\right)\left(\frac{71}{50}\right)\right]}e^{3t+2s}$, represented by a pink line. This comparison highlights the deviation between the

approximate and exact solutions, demonstrating the stability constraints required to maintain bounded differences. The visualization provides insight into the σ -semi–Ulam–Hyers stability behavior by show-casing how perturbations in the approximate solution evolve relative to the exact solution, ensuring that deviations remain controlled and well–regulated under the given stability framework.

Example 7.3. Consider the following NMPIDE with the condition:

$$\begin{cases}
\frac{\partial}{\partial s} \left[\frac{f(t,s) - se^{s} \left[\left(\frac{\sin(s)}{100} + 1 \right) \left(-6se^{s} \left[\log|t - 1| - 1 + t \log\left| \frac{t}{t - 1} \right| \right] (e^{s} - 1) - 1 \right) + 1 \right]}{\left(\frac{\sin(s)}{100} + 1 \right) f(t,s)} \\
= \frac{9}{s} \int_{0}^{1} \frac{2}{3} \log|t - \xi| f(\xi,s) d\xi, \\
f(t,0) = 0,
\end{cases} (63)$$

with $(t,s) \in [0,1] \times [0,1]$.

We verify that all the conditions of Theorem 5.1 are satisfied. The exact solution of the equation is known to be $f_0(t,s) = se^s$.

By comparing Equations (1) and (63) and performing some related mathematical computations, we obtain the following estimates:

$$\begin{split} &[a,b] = [0,1], \gamma = 9, \quad (t,s), (\xi,\tau) \in [0,1] \times [0,1]; \\ &h(t,s) = se^s \Big[\Big(\frac{\sin(s)}{100} + 1 \Big) \Big(-6se^s \Big[\log|t-1| - 1 + t \log \Big| \frac{t}{t-1} \Big| \Big] (e^s - 1) - 1 \Big) + 1 \Big], \\ &k(\alpha(s), f(t,s)) = \Big(\frac{\sin(s)}{100} + 1 \Big) f(t,s), \\ &\sup_{(t,s) \in [a,b] \times [a,b]} \Big| k(\alpha(s), f(t,s)) \Big| = \sup_{(t,s) \in [0,1] \times [0,1]} \Big| \Big(\frac{\sin(s)}{100} + 1 \Big) f(t,s) \Big| \le 30 = M; \end{split}$$

$$\phi(s) = \frac{1}{s}, \quad G(t, \xi) = \log|t - \xi|,$$
$$\left|\phi(\tau)G(t, \xi)\right| = \left|\frac{\log|t - \xi|}{\tau}\right| \le 1 = N;$$

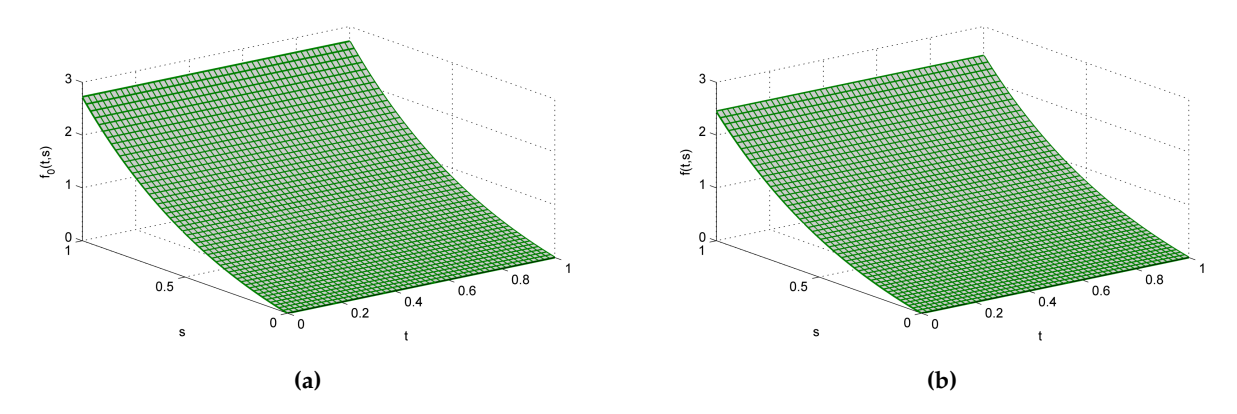


Figure 9: 3D Plots of the exact solution f_0 and the approximate solution f for Equation (63). These 3D plots illustrate the behavior of the exact solution f_0 and the approximate solution f over the domain $[0,1] \times [0,1]$. The visualization highlights the variations in both solutions as functions of two independent variables, providing a comprehensive perspective on their structural differences and similarities. Furthermore, the proximity of f to f_0 in the given domain underscores the stability properties of the approximate solution. In particular, the observed bounded deviation between f and f_0 aligns with the principles of Ulam–Hyers stability, reinforcing the reliability of the approximation within the prescribed interval.

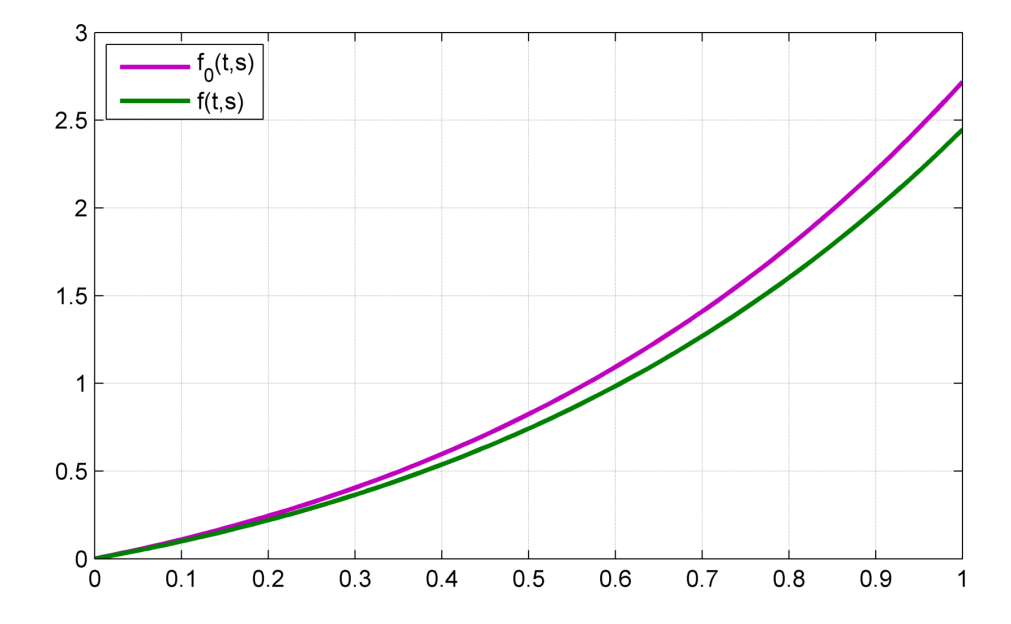


Figure 10: 2D plot of the exact solution f_0 and approximate solution f for Equation (63), visualizing their behavior over $[0,1] \times [0,1]$. The small deviation between f and f_0 confirms Ulam–Hyers stability, ensuring bounded perturbations and reliable approximation.

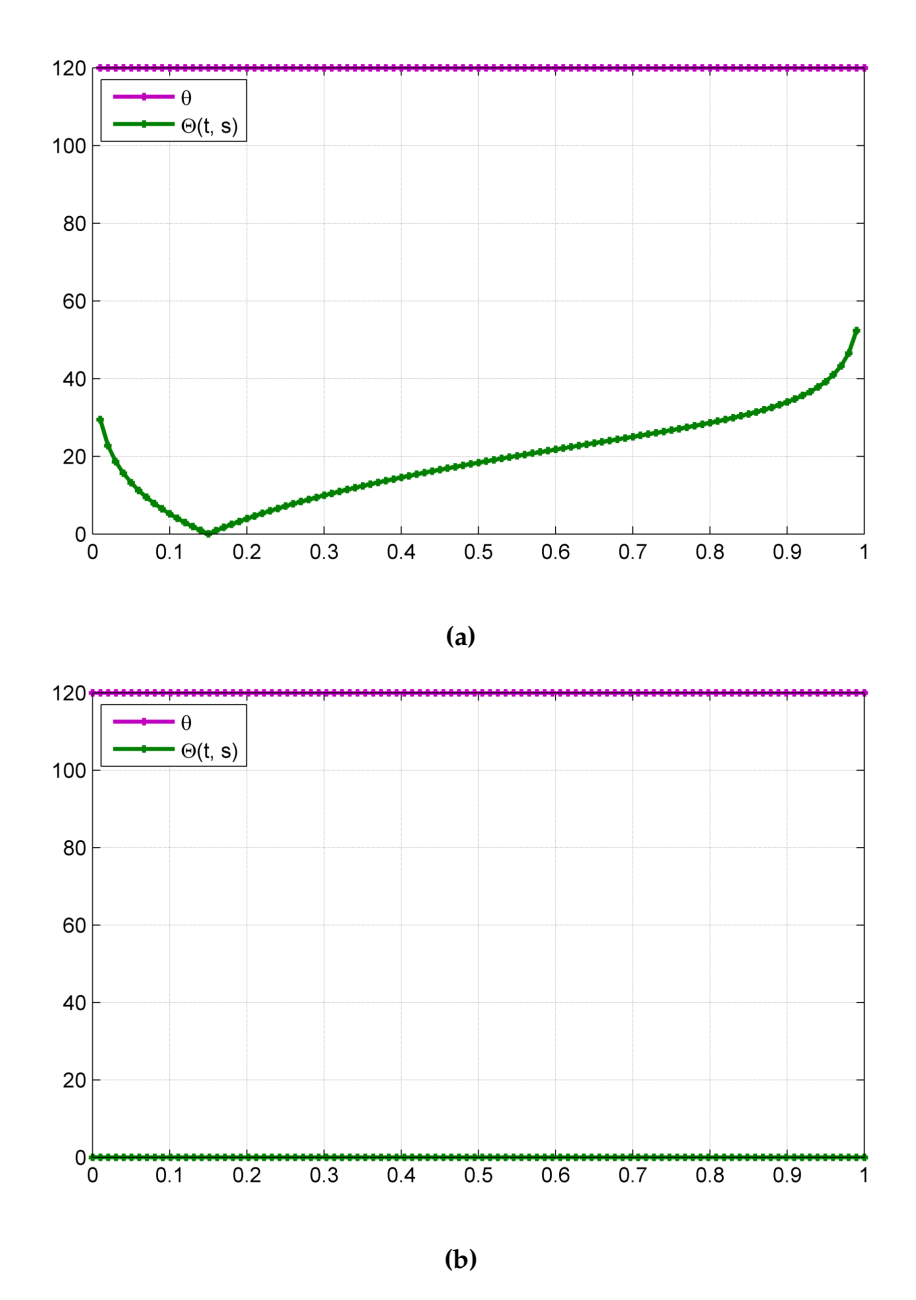


Figure 11: (a) 2D plot of the inequality (64) illustrating a comparison of $\Theta(t,s) = \left| \frac{100\cos(s)}{9(\sin(s)+100)^2} + \frac{60}{9} \left[\log|t-1| - 1 + t \log\left| \frac{t}{t-1} \right| \right] \left(e^{2s}(2s+1) - e^{s}(s+1) \right) - \frac{27e^{s}}{5} \left[\log|t| - 1 + t \log\left| \frac{t}{t-1} \right| \right] \right|$, represented by the green line, and the constant $\theta = 120$, represented by the pink line. This plot highlights the Ulam–Hyers stability by illustrating the bounded deviation; (b) 2D plot of the inequality (65) illustrating a comparison of $\Theta(t,s) = 0$, represented by the green line, and $\theta = 120$, represented by the pink line. The visualization emphasizes Ulam–Hyers stability by showcasing how the deviation remains controlled, ensuring stability in the considered framework.

$$\mu(t) = 0, \quad \Psi(f(\xi, \tau)) = \frac{2}{3}f(\xi, \tau),$$

$$\begin{split} \left| \Psi(f(\xi,\tau)) - \Psi(g(\xi,\tau)) \right| \\ &= \frac{2}{3} \left| f(\xi,\tau) - g(\xi,\tau) \right| \\ &\leq \frac{69}{100} \left| f(\xi,\tau) - g(\xi,\tau) \right| \\ &= L \left| f(\xi,\tau) - g(\xi,\tau) \right|, \, \forall \, f,g \in C^2([0,1] \times [0,1]). \end{split}$$

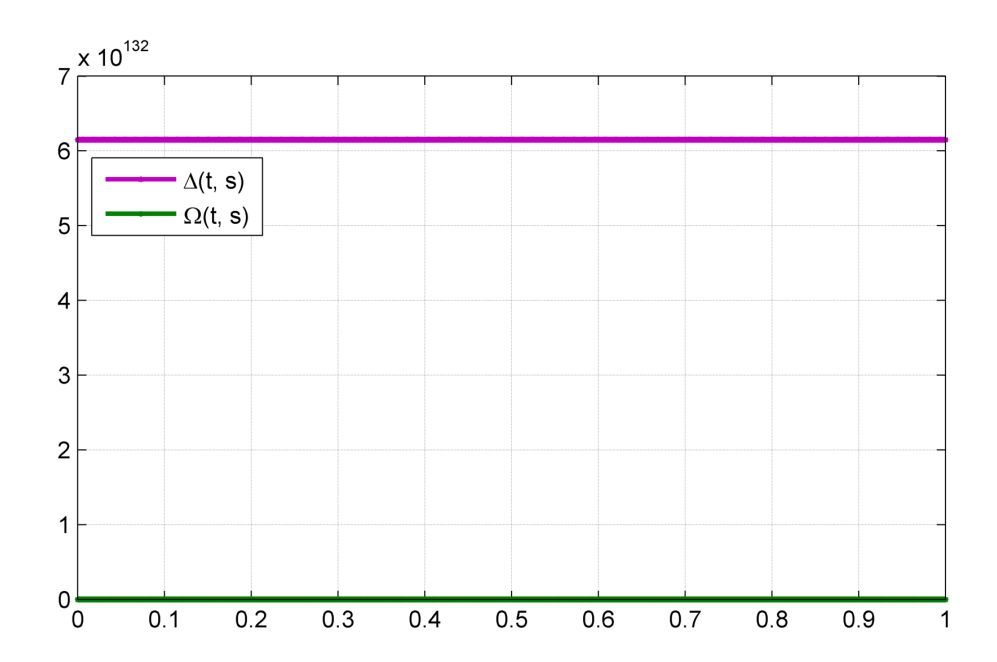


Figure 12: 2D plot of the inequality (66) illustrating that the deviation $\Omega(t,s) = \left|\frac{9}{10}se^s - se^s\right|$, representing the difference between the approximate and exact solutions, is bounded by the constant $\Delta(t,s) = \frac{(b-a)\sigma(b,b)}{(1-\beta N\gamma LM)\sigma(a,a)}\theta = \frac{120e^{300}}{[1-\frac{620}{1000}]}$, represented by the pink line. This visualization confirms that the approximation remains within a controlled bound, reinforcing the concept of Ulam–Hyers stability.

Moreover, we assume that there is $\beta > 0$, such that

$$\int_0^s \int_0^1 \sigma(\xi, \tau) \, d\xi d\tau = \int_0^s \int_0^1 e^{300\tau} \, d\xi d\tau \le \frac{e^{300s}}{300} = \beta \sigma(t, s),$$

where $\sigma(t,s) = e^{300s}$ is the nondecreasing continuous function. Using MATLAB, the exact solution f_0 and the approximate solution f of Equation (63) are illustrated in Fig. 9 and Fig. 10, respectively. If we choose $f(t,s) = \frac{9}{10}se^s$, it follows,

$$\left| \frac{\partial}{\partial s} \left[\frac{f(t,s) - h(t,s)}{k(\alpha(s), f(t,s))} \right] - \gamma \phi(s) \int_{0}^{1} G(t,\xi) \Psi(f(\xi,s)) d\xi \right|
= \left| \frac{100 \cos(s)}{9(\sin(s) + 100)^{2}} + \frac{60}{9} \left[\log|t - 1| - 1 + t \log\left|\frac{t}{t - 1}\right| \right] \left(e^{2s} (2s + 1) - e^{s} (s + 1) \right) - \frac{27e^{s}}{5} \left[\log|t| - 1 + t \log\left|\frac{t}{t - 1}\right| \right] \right| \le 120 = \theta,$$
(64)

$$|f(t,0) - \mu(t)| = 0 \le 120 = \theta,\tag{65}$$

where $(t,s) \in [0,1] \times [0,1]$. Fig. 11 shows the graphs of the functions from (64) and (65).

This demonstrates the Ulam–Hyers stability of the Equation (63). Furthermore, considering the exact solution $f_0(t,s) = se^s$ and the fact that $\beta N \gamma L M = 0.621 < 1$, we have

$$|f(t,s) - f_0(t,s)| = \left| \frac{9}{10} s e^s - s e^s \right|$$

$$\leq \frac{120 e^{300}}{\left[1 - \frac{621}{1000} \right]}$$

$$= \frac{(b-a)\sigma(b,b)}{(1-\beta N\gamma LM)\sigma(a,a)} \theta, \quad (t,s) \in [0,1] \times [0,1];$$
(66)

see Fig. 12.

Example 7.4. Consider the following NMPIDE with the condition:

$$\begin{cases}
\frac{\partial}{\partial s} \left[\frac{f(t,s) - \left((s^2 + 1) + \frac{\left(\frac{s^3}{3} + s \right)}{|t|^3} \right)}{\frac{74250 f(t,s)}{s^2 + 1}} \right] = \frac{1}{500} \left(\frac{1}{2} \right) \int_0^\infty \frac{1}{|t - \xi|^4} \left(\frac{4}{99} f(\xi, s) \right) d\xi, \\
f(t,0) = \frac{9}{10}.
\end{cases}$$
(67)

with $(t,s) \in [0,\infty) \times [0,\infty)$.

We confirm that all the conditions of Theorem 6.1 are fulfilled. The exact solution of the equation is known to be $f_0(t,s) = s^2 + 1$.

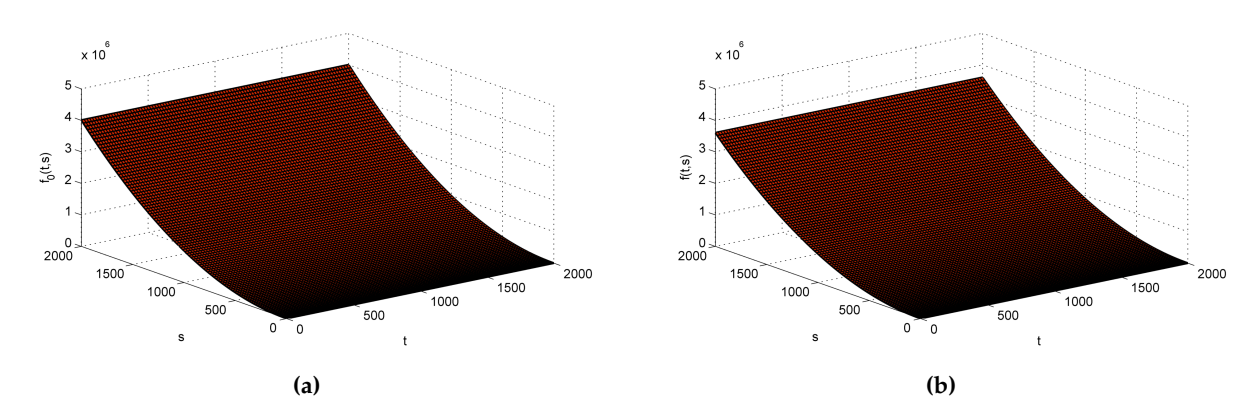


Figure 13: These 3D plots illustrate the exact solution f_0 and the approximate solution f for Equation (67), providing a detailed representation of their structural variations in three–dimensional space. The close agreement between f_0 and f highlights the bounded deviation, visually demonstrating the Ulam–Hyers–Rassias stability of the system. This depiction effectively captures the consistency between the solutions, reinforcing their interrelation.

By comparing Equations (1) and (67) and performing some related mathematical computations, we obtain the following estimates:

$$[a, \infty) = [0, \infty), \gamma = \frac{1}{500}, \quad (t, s), (\xi, \tau) \in [0, \infty) \times [0, \infty);$$

$$h(t,s) = (s^{2} + 1) + \frac{\left(\frac{s^{3}}{3} + s\right)}{|t|^{3}},$$

$$k(\alpha(s), f(t,s)) = \frac{74250 f(t,s)}{s^{2} + 1},$$

$$\sup_{(t,s) \in [a,\infty) \times [a,\infty)} \left| k(\alpha(s), f(t,s)) \right| = \sup_{(t,s) \in [0,\infty) \times [0,\infty)} \left| \frac{74250 f(t,s)}{s^{2} + 1} \right| \le 74250 = M;$$

$$\phi(s) = \frac{1}{2}, \quad G(t,\xi) = \frac{1}{|t - \xi|^{4}},$$

$$\left| \phi(\tau)G(t,\xi) \right| = \left| \frac{1}{2|t - \xi|^{4}} \right| \le \frac{1}{2} = N;$$

$$\mu(t) = \frac{9}{10}, \quad \Psi(f(\xi,\tau)) = \frac{4}{99} f(\xi,\tau),$$

$$\left| \Psi(f(\xi,\tau)) - \Psi(g(\xi,\tau)) \right|$$

$$= \left| \frac{4}{99} f(\xi,\tau) - \frac{4}{99} g(\xi,\tau) \right|$$

$$\le \frac{1}{20} \left| f(\xi,\tau) - g(\xi,\tau) \right|, \quad \forall f,g \in C_{b}^{2}([0,\infty) \times [0,\infty)).$$

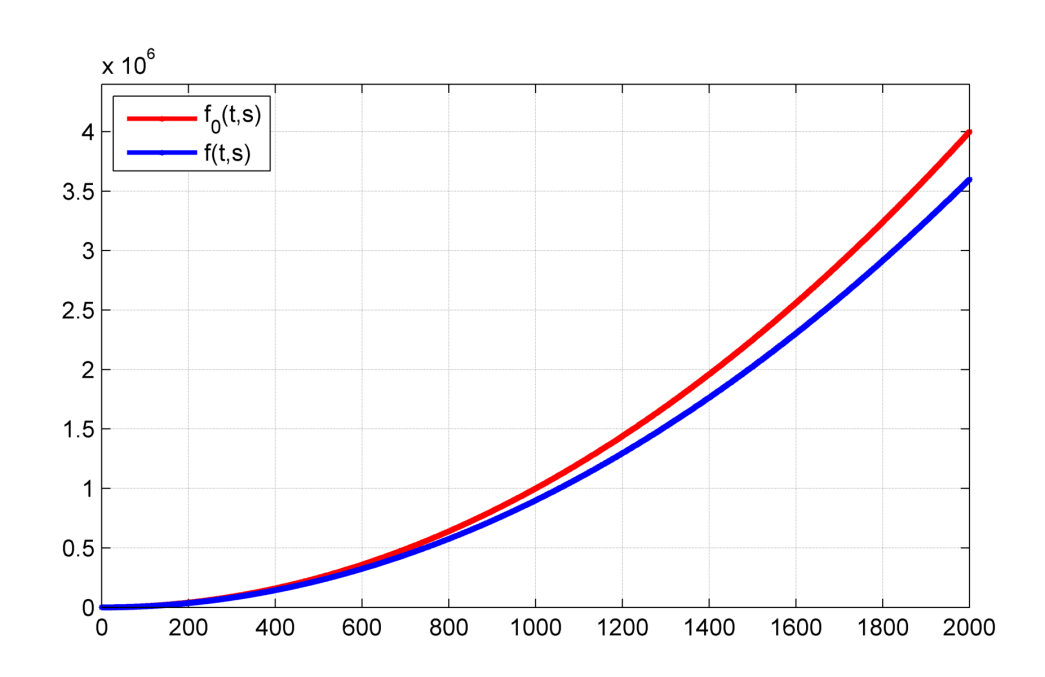
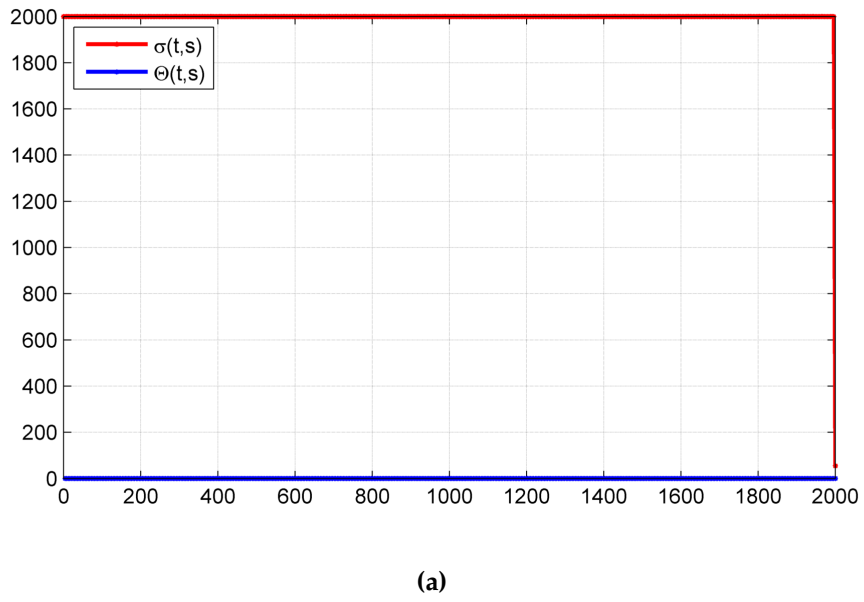


Figure 14: This 2D plot compares the exact solution f_0 and the approximate solution f of Equation (67), illustrating their closeness in the context of Ulam–Hyers–Rassias stability. The visualization highlights the stability property by demonstrating how the approximate solution remains bounded near the exact solution, reinforcing the robustness of the system under small perturbations.



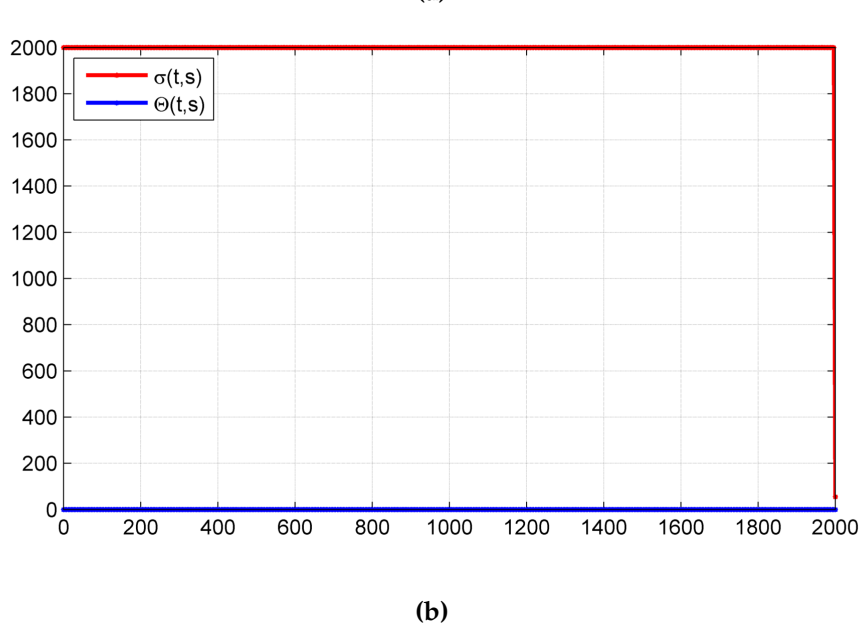


Figure 15: (a) 2D plot of the inequality (68), comparing the two functions: $\Theta(t,s) = \left| \frac{2s}{668250} + \frac{(s^2+1)}{6682500|t|^3} \right|$, denoted by a blue line, and $\sigma(t,s) = e^{-t+50s}$, denoted by a red line; (b) 2D plot of the inequality (69), comparing the functions: $\Theta(t,s) = 0$, denoted by a blue line, and $\sigma(t,s) = e^{-t+50s}$, denoted by a red line. These plots illustrate the bounded relationship between $\Theta(t,s)$ and $\sigma(t,s)$, demonstrating that deviations remain within a prescribed bound. This bounded behavior ensures Ulam–Hyers–Rassias stability, highlighting the system's resistance to perturbations. By visualizing these variations, the plots provide a clear representation of stability constraints, reinforcing the robustness of the system under small deviations.

Moreover, we assume that there is $\beta > 0$ *, such that*

$$\int_0^s \int_0^\infty \sigma(\xi,\tau)\,d\xi d\tau = \int_0^s \int_0^\infty e^{-\xi+50\tau}\,d\xi d\tau \leq \frac{1}{12} e^{-t+50s} = \beta \sigma(t,s),$$

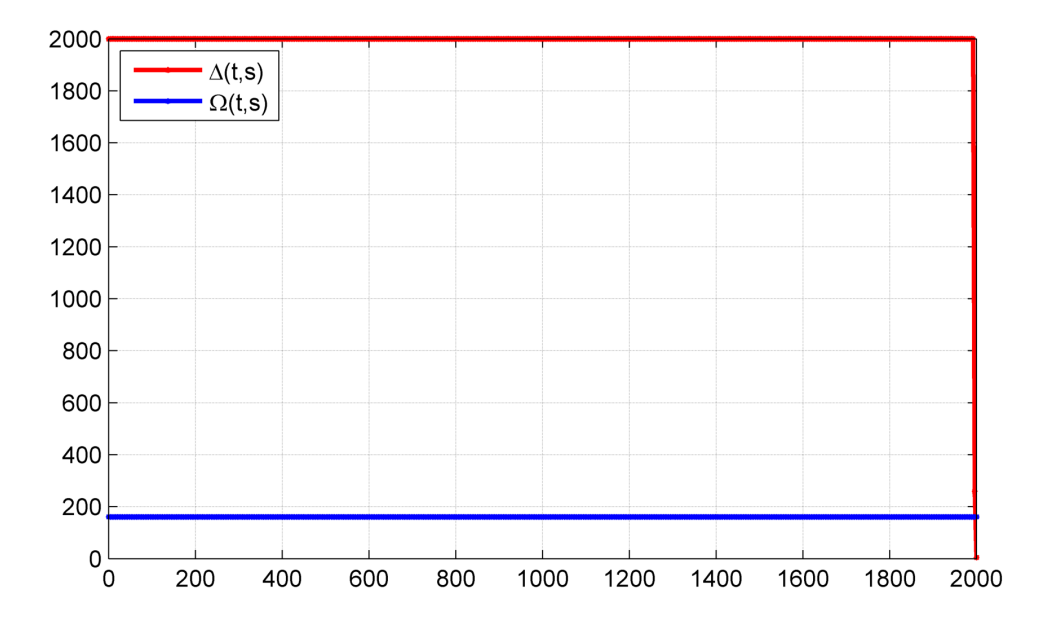


Figure 16: 2D plot of the inequality (70), illustrating a comparison between the two functions: $\Omega(t,s) = 0$ $\left|\frac{9}{10}(s^2+1)-(s^2+1)\right|$, denoted by a blue line, and $\Delta(t,s)=\frac{\beta}{1-\beta N\gamma LM}\sigma(t,s)=\frac{\beta}{1-\beta N\gamma LM}\sigma(t,s)$

denoted by a red line. This plot highlights their differing growth rates across the domain, where $\Omega(t,s)$ represents the deviation between the approximate and exact solutions. The function $\Delta(t,s)$ provides an upper bound for this deviation, ensuring Ulam-Hyers-Rassias stability, meaning that the approximation error remains controlled and does not diverge significantly from the exact solution. The exponential decay in $\Delta(t, s)$ further supports the stability of the system.

where $\sigma(t,s) = e^{-t+50s}$ is the nondecreasing continuous function. Using MATLAB, the exact solution f_0 and the approximate solution f_0 of Equation (67) are illustrated in Figs. 13 and 14. If we choose $f(t,s) = \frac{9}{10}(s^2+1)$, it follows,

$$\left| \frac{\partial}{\partial s} \left[\frac{f(t,s) - h(t,s)}{k(\alpha(s), f(t,s))} \right] - \gamma \phi(s) \int_0^\infty G(t,\xi) \Psi(f(\xi,s)) d\xi \right|$$

$$= \left| \frac{2s}{668250} + \frac{(s^2 + 1)}{6682500|t|^3} \right| \le e^{-t + 50s} = \sigma(t,s),$$
(68)

$$|f(t,0) - \mu(t)| = 0 \le e^{-t+50s} = \sigma(t,s),$$
 (69)

where $(t,s) \in [0,\infty) \times [0,\infty)$. Fig. 15 represents the graphs of the functions appearing in (68) and (69).

This demonstrates the Ulam-Hyers-Rassias stability of the Equation (67). Furthermore, considering the exact solution $f_0(t,s) = (s^2 + 1)$ and the fact that $\beta N \gamma L M = 0.3094 < 1$, we have

$$\left| f(t,s) - f_0(t,s) \right| = \left| \frac{9}{10} (s^2 + 1) - (s^2 + 1) \right|
\leq \frac{1}{12 \left[1 - \left(\frac{1}{12} \right) \left(\frac{1}{20} \right) \left(\frac{1}{200} \right) \left(74250 \right) \right]} e^{-t + 50s}
= \frac{\beta}{1 - \beta N \gamma L M} \sigma(t,s), \quad (t,s) \in [0,\infty) \times [0,\infty);$$
(70)

see Fig. 16.

8. Conclusions and Future Direction

This study marks a crucial step in analyzing the stability of NMPIDEs with discontinuous kernels. For the first time, we have rigorously applied Ulam–Hyers and Ulam–Hyers–Rassias criteria to these equations, offering valuable insights into how discontinuous kernels influence system stability. Using fixed–point arguments within continuous function spaces and the generalized Bielecki metric, we have provided a detailed framework that clarifies the conditions required for stability and highlights the complex behavior introduced by discontinuous elements.

In addition to this foundational analysis, we also explored the concept of σ -semi–Ulam–Hyers stability, shedding light on how slight perturbations affect the stability of the system. This extension is vital for understanding how stability behaves under small disturbances, providing a broader perspective on the overall stability of the system.

Future research can build on these findings by investigating Ulam–Hyers–Mittag–Leffler stability, a promising direction that could further enhance our understanding of stability for these equations. By incorporating Mittag–Leffler functions, we may discover new stability criteria that deepen our insights and broaden the applicability of the results to a wider class of equations.

The exploration of these open problems could lead to significant advancements in both theory and practical applications. Addressing such challenges offers a pathway to improve the analysis of complex systems with discontinuous kernels, with potential applications in various scientific fields.

This work provides a novel and comprehensive analysis of stability using Ulam–Hyers, Ulam–Hyers–Rassias, and σ –semi–Ulam–Hyers stability, laying the groundwork for future studies. Expanding the investigation to include Ulam–Hyers–Mittag–Leffler stability and other extensions will further enrich the field and contribute to the development of new mathematical tools and applications.

Ethics declarations

Conflict of interest

The authors declare that they have no conflicts of interest.

Fundings

No funding was used in this study.

References

- A. M. Al-Bugami, M. A. Abdou, A. M. S. Mahdy, Numerical Simulation, Existence and Uniqueness for Solving Nonlinear Mixed Partial Integro-Differential Equations with Discontinuous Kernels, J. Appl. Math. Comput. (2024). https://doi.org/10.1007/s12190-024-02160-x
- [2] A. Selvam, S. Sabarinathan, S. Pinelas, *The Aboodh transform techniques to Ulam type stability of linear delay differential equation*, Int. J. Appl. Comput. Math. **9** (2023), 115. https://doi.org/10.1007/s40819-023-01577-5.
- [3] A. Selvam, S. Sabarinathan, S. Noeiaghdam, V. Govindan, Fractional Fourier transform and Ulam stability of fractional differential equation with fractional Caputo-type derivative, J. Funct. Spaces 2022 (2022), 5. https://doi.org/10.1155/2022/3777566.
- [4] A. Selvam, S. Sabarinathan, B. V. S. Kumar, H. Byeon, K. Guedri, S. M. Eldin, M. I. Khan, V. Govindan, *Ulam–Hyers stability of tuberculosis and COVID–19 co–infection model under Atangana-Baleanu fractal–fractional operator*, Sci. Rep. 13 (2023), 9012. https://doi.org/10.1038/s41598-023-35624-4.
- [5] A. Turab, W. Sintunavarat, On analytic model for two-choice behavior of the paradise fish based on the fixed point method, J. Fixed Point Theory Appl. 21 (2019), 56. https://doi.org/10.1007/s11784-019-0694-y.
- [6] A. Turab, W. Sintunavarat, The novel existence results of solutions for a nonlinear fractional boundary value problem on the ethane graph, Alex. Eng. J. 60 (2021), no. 6, 5365–5374. https://doi.org/10.1016/j.aej.2021.04.020.
- [7] A. Turab, W. Sintunavarat, On the solution of the traumatic avoidance learning model approached by the Banach fixed point theorem, J. Fixed Point Theory Appl. 22 (2020), 50. https://doi.org/10.1007/s11784-020-00788-3.
- [8] A. M. Simões, Different stabilities for oscillatory Volterra integral equations, Math. Meth. Appl. Sci. 46 (2023), no. 9, 9942–9953. https://doi.org/10.1002/mma.9094.
- [9] A. Zada, W. Ali, S. Farina, Hyers Ulam Stability of Nonlinear Differential Equations with Fractional Integrable Impulses, Math. Methods Appl. Sci. 40 (2017), 5502–5514. https://doi.org/10.1002/mma.4405.

- [10] C. C. Tisdell, A. Zaidi, Basic Qualitative and Quantitative Results for Solutions to Nonlinear, Dynamic Equations on Time Scales with an Application to Economic Modelling, Nonlinear Anal. 68 (2008), no. 11, 3504–3524. https://doi.org/10.1016/j.na.2007.03.043.
- [11] D. H. Hyers, On the stability of the linear functional equation, Proc. Natl. Acad. Sci. USA 27 (1941), no. 4, 222–224. https://doi.org/10.1073/pnas.27.4.222.
- [12] D. Marian, S. A. Ciplea, N. Lungu, *Ulam–Hyers Stability of a Parabolic Partial Differential Equation*, Demonstr. Math. **52** (2019), no. 1, 475–481. https://doi.org/10.1515/dema-2019-0040.
- [13] D. Pachaiyappan, R. Murali, C. Park, J. R. Lee, Relation between electrical resistance and conductance using multifarious functional equations and applications to parallel circuit, J. Inequal. Appl. 2022 (2022), 60. https://doi.org/10.1186/s13660-022-02795-z.
- [14] E. Karapinar, R. P. Agarwal, Fixed Point Theory in Generalized Metric Spaces, Synth. Lect. Math. Stat., Springer (2022).
- [15] H. Rezaei, S. M. Jung, T. M. Rassias, Laplace transform and Hyers–Ulam stability of linear differential equations, J. Math. Anal. Appl. 403 (2013), no. 1, 244–251. https://doi.org/10.1016/j.jmaa.2013.02.034.
- [16] J. Brzdęk, J. Chudziak, Z. Páles, A Fixed Point Approach to Stability of Functional Equations, Nonlinear Anal. 74 (2011), no. 17, 6728–6732. https://doi.org/10.1016/j.na.2011.06.052.
- [17] J. Wang, Y. Zhang, A Class of Nonlinear Differential Equations with Fractional Integrable Impulses, Com. Nonl. Sci. Num. Sim. 19 (2014), no. 9, 3001–3010. https://doi.org/10.1016/j.cnsns.2014.01.016.
- [18] J. B. Diaz, B. Margolis, A Fixed Point Theorem of the Alternative, for Contractions on a Generalized Complete Metric Space, Bull. Am. Math. Soc. 74 (1968), 305–309.
- [19] K. Ciepliński, *Applications of Fixed Point Theorems to the Hyers–Ulam Stability of Functional Equations—A Survey*, Ann. Funct. Anal. **3** (2012), no. 1, 151–164. 10.15352/afa/1399900032.
- [20] L. Yin, Z. Geng, A. Björneklett, E. Söderlund, T. Thiringer, D. Brandell, An integrated flow electric thermal model for a cylindrical Li–I on battery module with a direct liquid cooling strategy, Energy Technol. 10 (2022), 2101131. https://doi.org/10.1002/ente.202101131.
- [21] L. P. Castro, A. M. Simões, Different Types of Hyers–Ulam–Rassias Stabilities for a Class of Integro-Differential Equations, Filomat 31 (2017), no. 17, 5379–5390. 10.2298/FIL1717379C.
- [22] L. P. Castro, A. M. Simões, Hyers–Ulam and Hyers–Ulam–Rassias Stability of a Class of Hammerstein Integral Equations, AIP Conf. Proc. 1798 (2017), no. 1, 020036. 10.1063/1.4972628.
- [23] L. Cădariu, L. Găvruța, P. Găvruța, Weighted Space Method for the Stability of Some Nonlinear Equations, Appl. Anal. Discrete Math. 6 (2012), no. 1, 126–139.
- [24] L. Cădariu, V. Radu, Fixed Points and the Stability of Jensen's Functional Equation, J. Inequal. Pure Appl. Math. 4 (2003), 4.
- [25] M. Sivashankar, S. Sabarinathan, K. S. Nisar, C. Ravichandran, B. V. S. Kumar, Some properties and stability of Helmholtz model involved with nonlinear fractional difference equations and its relevance with quadcopter, Chaos Solitons Fract. 168 (2023), 113161. https://doi.org/10.1016/j.chaos.2023.113161.
- [26] M. Sivashankar, S. Sabarinathan, V. Govindan, U. Fernandez-Gamiz, S. Noeiaghdam, Stability analysis of COVID-19 outbreak using Caputo-Fabrizio fractional differential equation, Aims Math. 8 (2023), 2720–2735. https://doi.org/10.3934/math.2023143.
- [27] M. Akkouchi, Hyers–Ulam–Rassias Stability of Nonlinear Volterra Integral Equations via a Fixed Point Approach, Acta Univ. Apulensis Math. Inform. 26 (2011), 257–266.
- [28] N. Khan, Z. Ahmad, J. Shah, S. Murtaza, M. D. Albalwi, H. Ahmad, J. Baili, S. W. Yao, Dynamics of chaotic system based on circuit design with Ulam stability through fractal-fractional derivative with power law kernel, Sci. Rep. 13 (2023), 5043. https://doi.org/10.1038/s41598-023-32099-1.
- [29] R. Shah et al., Stability of Hybrid Differential Equations in the Sense of Hyers–Ulam Using Gronwall Lemma, Filomat 39 (2025), no. 4, 1407–1417. https://doi.org/10.2298/FIL2504407S.
- [30] R. Ghania, L. Mchiri, M. Rhaima, M. Hannabou, A. Ben Makhlouf, Stability Results for the Darboux Problem of Conformable Partial Differential Equations, Axioms 12 (2023), no. 7, 640. https://doi.org/10.3390/axioms12070640.
- [31] R. Murali, A. P. Selvan, C. Park, Ulam stability of linear differential equations using Fourier transform, Aims Math. 5 (2020), 766–780.
- [32] R. Shah, A. Zada, Hyers–Ulam–Rassias stability of impulsive Volterra integral equation via a fixed point approach, J. Linear Topol. Algebra 8 (2019), no. 4, 219–227.
- [33] R. Shah, A. Zada, A fixed point approach to the stability of a nonlinear Volterra integrodifferential equation with delay, Hacet. J. Math. Stat. 47 (2018), no. 3, 615–623. https://doi.org/10.15672/HJMS.2017.467.
- [34] R. Shah, E. Tanveer, *Ulam–type stabilities for* (k, ψ) *–fractional order quadratic integral equations*, Filomat **39** (2025), no. 7, 2457–2473. https://doi.org/10.2298/FIL2507457S.
- [35] R. Shah, H. I. Abbasi, Hyers–Ullam stability for Hammerstein integral equations with impulses and delay, Filomat 39 (2025), no. 7, 2417–2428. https://doi.org/10.2298/FIL2507417S.
- [36] R. Shah, E. Tanveer, *Ulam—Hyers stability of higher dimensional weakly singular Volterra integral equations*, Filomat **39** (2025), no. 7, 2429–2437. https://doi.org/10.2298/FIL2507429S.
- [37] R. Shah, L. Wajid, Z. Hameed, Hyers-Ulam stability of non-linear Volterra-Fredholm integro-differential equations via successive approximation method, Filomat 39 (2025), no. 7, 2385–2404. https://doi.org/10.2298/FIL2507385S.
- [38] R. Shah, H. Bibi, N. Irshad, H. I. Abbasi, On Hyers–Ulam stability of a class of impulsive Hammerstein integral equations, Filomat 39 (2025), no. 7, 2405–2416. https://doi.org/10.2298/FIL2507405S.
- [39] R. Shah, N. Irshad, On the Hyers–Ulam stability of Bernoulli's differential equation, Russ. Math. 68 (2024), no. 12, 17–24. https://doi.org/10.3103/S1066369X23600637.
- [40] R. Shah, N. Irshad, Ulam—Hyers—Mittag—Leffler stability for a class of nonlinear fractional reaction—diffusion equations with delay, Int. J. Theor. Phys. 64 (2025), no. 20. https://doi.org/10.1007/s10773-025-05884-z.
- [41] R. Shah, N. Irshad, H. I. Abbasi, Hyers–Ulam–Rassias stability of impulsive Fredholm integral equations on finite intervals, Filomat 39 (2025), no. 2, 697–713. https://doi.org/10.2298/FIL2502697S.
- [42] R. Shah, N. Irshad, Ulam type stabilities for oscillatory Volterra integral equations, Filomat 39 (2025), no. 3, 989–996. https://doi.org/10.2298/FIL2503989S.

- [43] S. M. Ulam, Problems in Modern Mathematics, Wiley, New York, USA, 1964.
- [44] S. M. Ulam, A Collection of Mathematical Problems, Intersci. Publ., New York-London, 8 (1960).
- [45] S. Lin, Z. Yun, Generalized Metric Spaces and Mappings, Atlantis Stud. Math., Amsterdam: Atlantis Press, (2016).
- [46] S. Şevgina, H. Şevlib, Stability of a nonlinear Volterra integro–differential equation via a fixed point approach, J. Nonlinear Sci. Appl. 9 (2016), no. 1, 200–207. https://doi.org/10.22436/jnsa.009.01.18.
- [47] T. Aoki, On the stability of the linear transformation in Banach spaces, J. Math. Soc. Japan 2 (1950), no. 1–2, 64–66. https://doi.org/10.2969/jmsj/00210064.
- [48] T. M. Rassias, On the stability of the linear mapping in Banach spaces, Proc. Am. Math. Soc. 72 (1978), no. 2, 297–300. https://doi.org/10.2307/2042795.
- [49] V. Kalvandi, N. Eghbali, J. M. Rassias, Mittag–Leffler–Hyers–Ulam stability of fractional differential equations of second order, J. Math. Ext. 13 (2019), 29–43.
- [50] V. Radu, The Fixed Point Alternative and the Stability of Functional Equations, Fixed Point Theory 4 (2003), 91–96.
- [51] Z. Lin, W. Wei, J. Wang, Existence and stability results for impulsive integro–differential equations, Facta Univ. Ser. Math. Inform. 29 (2015), no. 2, 119–130.
- [52] Z. Gajda, On Stability of Additive Mappings, Internat. J. Math. Math. Sci. 14 (1991), 431–434. https://doi.org/10.1155/S016117129100056X.